Annals of Operations Research
https://doi.org/10.1007/s10479-026-07071-7

ORIGINAL RESEARCH

Assessing climate risk on the European financial system: a multi-scenario Analysis

Gianandrea Giacchetta[1] · **Rosella Giacometti**[1] · **Gabriele Torri**[1,2]

Received: 3 May 2025 / Accepted: 20 January 2026

Abstract
This paper investigates the impact of climate risk on the stability of the European financial system, with a particular focus on both transition and physical risk dimensions. Given the long-term and uncertain nature of climate-related risks, traditional econometric methods often fall short in capturing their systemic implications. To address this challenge, we develop a scenario-based framework grounded in realistic projections consistent to the theoretical framework of the Network for Greening the Financial System ("NGFS"), encompassing three climate pathways: orderly transition, disorderly transition, and hot house world. We model the relationship between climate risk drivers, European companies, and the financial system using vine copulas, enabling a flexible representation of complex dependencies. The effects of these scenarios on financial institutions are evaluated through key risk metrics (expected return, value at risk, and expected shortfall) conditioned on each climate scenario. Our results offer insights into how climate transition risks propagate through the financial system, with practical implications for financial stability assessment and systemic risk management. The primary contribution lies in integrating both transition and physical climate risks into a coherent and tractable risk assessment framework, offering valuable tools for policymakers, regulators, and financial practitioners. Results show a significant dependence of European financial system to brown companies and, thus, sizable losses in the disorderly transition scenario.

Keywords Climate finance · Transition risk · Physical risk · Climate stress testing · Copula

✉ Gianandrea Giacchetta
gianandrea.giacchetta@unibg.it

Rosella Giacometti
rosella.giacometti@unibg.it

Gabriele Torri
gabriele.torri@unibg.it

[1] Department of Economics, University of Bergamo, Via dei Caniana, 2, Bergamo 24127, BG, Italy

[2] Department of Finance, VSB-Technical University of Ostrava, 17. listopadu 2172/15, Ostrava 70800, Moravian-Silesian, Czech Republic

Published online: 07 February 2026

1 Introduction

Globally, 2024 was the warmest year ever recorded and it is documented that the average global mean near-surface temperature in 2024 exceeded pre-industrial levels by 1.55°C (WMO, 2025). The impact of climate change is so tremendously tangible that it represents one of the most prominent challenges of our century and it is becoming increasingly urgent to find an agreed-upon strategy to mitigate its potential negative consequences.

From a financial perspective, the transition to a low-carbon economy and the rising threat of extreme weather events involve risks that might worsen the performance of firms, with potential spillovers for financial stability (see for example Barnett, 2023).

Financial supervisors have identified two main categories of climate risks (Alogoskoufis et al., 2021a): (i) risks related to the *transition* to a lower carbon economy (*transition risks*) and (ii) risks related to the *physical* impacts of climate change (*physical risks*). Transition risks stem from policy measures and regulatory actions aimed at reducing carbon emissions and typically encompass policy and legal risks, technological risks, market risks, and reputational risks. By contrast, physical risks derive from the potential damages caused by acute or chronic climate events, such as hurricanes, floods, and droughts.

Companies and investors are exposed to a balance of transition and physical risks. This trade-off is particularly relevant from a policy perspective. Aggressive actions to limit climate change to below 2°C, in accordance with the Paris Agreement, would likely increase transition risks whilst reducing physical risks globally. Conversely, limited actions to reduce GHG emissions would limit key transition risks, but would result in accelerating climate change and associated physical risks (Lord et al., 2019).

Financial institutions have limited ability to alter the trajectory of climate scenarios themselves, which are determined by broader socio-economic, technological, and policy developments. Nevertheless, systematic analysis of alternative scenarios can provide valuable insights into the range and scale of potential impacts on portfolios and balance sheets. In this sense, while banks cannot influence the evolution of climate pathways, they can adapt their operational strategies and risk-management frameworks in response to the projected consequences of those scenarios.

Many efforts are being carried by central banks, regulators and investors on evaluating the impact of climate transition and physical risks on financial firms and, more broadly, on the stability of the financial system (see for example Carney 2015 and Campiglio et al. 2018)

Recently, central banks have started including climate stress tests in their annual supervisory framework (Alogoskoufis et al., 2021b; Dunz et al., 2021). The concept of stress test commonly indicates a set of analytical techniques and exercises used to study the relationships between variables in extreme situations and explore potential impacts of systemic events. According to the Financial Stability Board, "*a systemic event is the disruption to the flow of financial services that is (i) caused by an impairment of all or parts of the financial system and (ii) has the potential to have serious negative consequences on the real economy*" (Financial Stability Board, 2009). In that sense, climate-related risks can plausibly be counted as systemic events.

The pioneering work of Battiston et al. (2017) proposed the first climate stress test to consider spillover effects within the banking sector. In particular, authors developed an innovative network-based climate stress-test methodology and applied it to large Euro Area banks in a "green" and a "brown" scenario. Results revealed both a direct and indirect exposure to climate-policy relevant sectors. Roncoroni et al. (2021) extended this approach to include also investment funds. Several methodological approaches have been then proposed for cli-

mate stress testing and, more specifically, for assessing climate transition risk (Le Guenedal, 2022; Desnos et al., 2023).

While there is a growing strand of literature that contributes to forecast the impact of transition risk on the financial system, the climate physical risk remains comparatively underexplored and only partially addressed (some recent works include Addoum et al. 2020, Ardia et al. 2023, Sautner et al. 2023 and Albanese et al. 2024). As reported by Rising et al. (2022), this is primary due to a couple of reasons. First, there is an evident time lag between the analysis of physical risks, economic understanding of the implications of those physical risks and their nonlinear social feedbacks, and embodiment of that knowledge in an economic model or analysis. Second, incomplete understanding and high uncertainty of the physical processes may encourage scientists either to be conservative in characterizing them or focus on their central estimates. Moreover, physical risk often deals with variables that are not strictly economic or financial ones, which involve the analysis of long-term time series of extreme weather events.

Building on the recent climate finance literature, the aim of this paper is to assess the resilience of European financial institutions to climate-related risks by applying climate stress-testing methodologies across multiple climate scenarios. For a comprehensive discussion of existing approaches and challenges in this area, see Acharya et al. (2023).

Expanding from Ojea-Ferreiro et al. (2024), we develop an empirical set-up that allows the quantification of the effects of climate risk on financial institutions. Differently from Ojea-Ferreiro et al. (2024), we account not only for the climate transition risk, but also for the climate physical risk, which impact can potentially affect the financial system as much as the transition risk. Conceptually, the analysis is similar to models that measure systemic risk using conditional distributions to account for tail risk interconnectedness, such as CoVaR (Tobias and Brunnermeier, 2016), or Marginal Expected Shortfall (Acharya et al., 2017), with the difference that in our work the conditioning factors are calibrated on specific climate scenarios rather than states of market distress.

Typically, climate finance literature addresses transition and physical risk separately (see for example Tzouvanas et al., 2019). We argue that the conventional separation of analyses between transition and physical climate risks neglects the potential interactions between their respective drivers and impacts, thereby resulting in an underestimation of potential losses at the level of firms, financial institutions, and the broader economy. Accordingly, in this paper we seek to account for the interdependencies between these two categories of risks in order to obtain a holistic assessment of banks' climate-related exposure and to evaluate the compounded effects of multiple risk factors. The effects produced by the interaction between variables which differ in nature is not obvious.

Concretely, we apply scenario analysis by modeling the conditional distribution of financial firm returns under three climate scenarios, namely *disorderly transition*, *hot house world* and *orderly transition*. The scenario set-up is NGFS-aligned, meaning that assumed climate scenarios are consistent with the theoretical framework presented by the Network for Greening the Financial System ("NGFS"), one of the most authoritative and used in literature.

In this work, we estimate the effect of climate shocks on a representative sample of 43 European banks by employing a set of random variables that proxy transition and physical climate risk. Our probabilistic approach enables the estimation of climate impact on stock returns at a weekly frequency, relying on a parsimonious set of variables, despite the dependence of NGFS climate scenario to long-term climate trends. Moreover, it does not require granular data of banks' exposures to model the transmission of shocks from the real economy to the banking sector. The probability of each scenario is defined through the joint probability distribution of a set of factors which mimic the dynamic of transition and physical risks.

In the literature, the study of climate physical risk involves variables falling beyond the typical economist's knowledge and expertise, such as dynamic of temperature, intensity of winds and precipitation, droughts and many others. We thus rely on a physical risk index, the European Events Climate Index (E^3CI), developed by a pool of research centers and private entities[1]. Transition risk, in line with Ojea-Ferreiro et al. (2024), is proxied by the relative dynamics of "green" and "brown" company performance (classified according to their greenhouse gas emissions), as these firms are expected to react differently under alternative climate scenarios: in the hot house world scenario, brown and green assets experience upward and downward movements, respectively; in the disorderly transition scenario, we assume the opposite behavior, *i.e.* green and brown assets experience upward and downward movements, respectively; finally, in an orderly transition scenario, green, neutral, and brown asset values remain stably in and around their median values.

Once the climate risk drivers are identified, we evaluate the impact of each climate scenario on the return of banks in terms of the average of the conditional distribution, a low quantile of the conditional distribution and the average in the lower tail of the conditional distribution, named respectively as climate expected return (C-ER), climate value at risk (C-VAR) and climate expected shortfall (C-ES). The three metrics are computed for individual financial firms relying on conditional copula functions that characterize dependencies between financial firms, physical risk index and "green" and "brown" asset returns. The methodology is applied on a sample of the most representative banks of the European financial system.

In the last part of the paper, after computing the systemic risk metrics aforementioned, we assess the impact of climate-related systemic risk on financial institutions, focusing on capital shortfalls following Acharya et al. (2017) and Brownlees and Engle (2017). With regard to banks, our analysis points out that the capital shortfall under the hot house world scenario is negligible. On the other hand, under the disorderly transition and orderly transition scenarios, we observe non-negligible substantial capital shortfalls. This outcome poses a material concern for the European financial system, since the policy trajectory now being followed by governments is explicitly towards a low-carbon economy. Whether the transition occurs orderly or disorderly, banks will face capital pressure, so the most likely policy-driven scenarios are also those under which the system is most vulnerable. However, capital shortfalls involve only a few institutions and stay manageable at the system-wide level in the banking sector. These topics are nowadays considered of great relevance from both a regulatory and an investor's point of view. From a regulatory perspective, identifying the banks that are most exposed to climate risk under stress scenarios may contribute to strengthen the European financial system. From an investor's point of view, understanding whether climate-related factors are material to creditworthiness is crucial to assess the true cost of banks' debt and the embedded risk premium, helping them make more informed investment decisions.

2 Climate scenarios

To provide a standard source of information, the NGFS has selected a set of models and variables that best suit the transition to a greener economy (NGFS, 2022). Starting from 2020, the NGFS has been projecting and updating different trajectories of climate evolution.

[1] For more information about the E^3CI Index, please refer to https://climateindex.eu/.

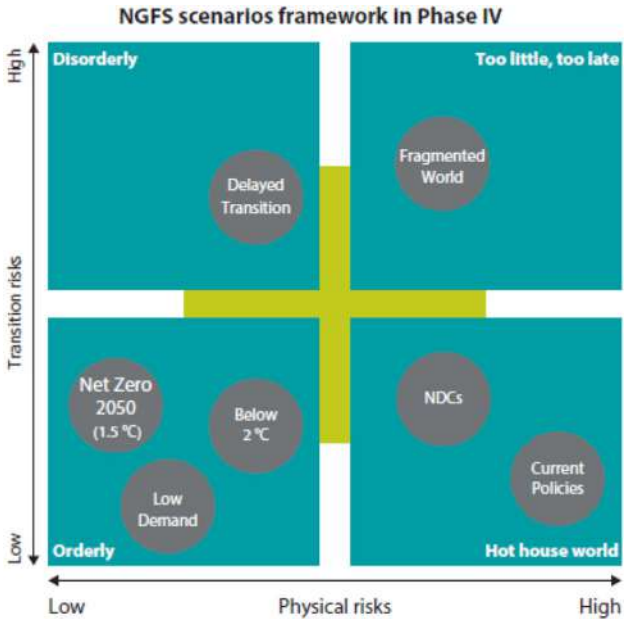

Fig. 1 Physical and transition risk level of NGFS scenarios . Source: NGFS (2022). Positioning of scenarios is approximate, based on an assessment of physical and transition risks out to 2100. **1. Orderly scenarios:** Assume climate policies are introduced early and become gradually more stringent. Both physical and transition risks are relatively subdued. **2. Disorderly scenarios:** Explore higher transition risk due to policies being delayed or divergent across countries and sectors. Carbon prices are typically higher for a given temperature outcome. These scenarios typically assume the introduction of climate policies starting from 2030, with a country differentiation based on currently implemented policies. **3. Hot house world scenarios:** Assume that some climate policies are implemented in some jurisdictions, but global efforts are insufficient to halt significant global warming. Critical temperature thresholds are exceeded, leading to severe physical risks and irreversible impacts like sea-level rise. **4. Too little, too late scenarios:** Reflect delays and international divergences in climate policy ambition that imply elevated transition risks in some countries and high physical risks in all countries due to the overall ineffectiveness of the transition.

Each trajectory is represented by a climate scenario[2]. The seven assumed scenarios[3] represent all outcomes with their underlying hypothesis, which add complexity to asset pricing in the context of climate scenario uncertainty. Eventually, the NGFS framework depicts climate scenarios on a cartesian plane, with transition and physical risks represented on the two axes, and the resulting combinations grouped into four quadrants, as represented in Fig. 1.

Each quadrant denotes a different combination of transition and physical risk. We remark that the NGFS does not assess the likelihood of each scenario; instead, they "aim at exploring the bookends of plausible futures (neither the most probable nor desirable) for financial risk assessment" (Boirard et al., 2022). Recent works (see for example Ojea-Ferreiro et al., 2024) have tried to model climate-related scenarios through a copula approach, on the assumption that different climate trajectories correspond to different impacts on values of

[2] NGFS defines a climate scenario as a plausible description of how the future may develop based on a coherent and internally consistent set of assumptions about key driving forces (e.g., rate of technological change, prices) and relationships. Note that scenarios are neither predictions nor forecasts, but are used to provide a view of the implications of developments and actions.

[3] Namely, *Delayed Transition*, *Net Zero 2050*, *Below* 2°*C*, *Low Demand*, *Fragmented World*, *NDCs* and *Current Policies*.

assets depending on their transition risk exposure. For instance, when introducing new green policies, green companies and brown companies are likely to experience a stock price increase and decrease respectively, such that each scenario can be characterized in terms of the joint movement of stocks' returns of companies.

In order to be NGFS-consistent, we introduce the physical risk dimension along with the transition one. In doing that, still it is possible to attribute scenario-related probabilities with a copula approach, by assuming a hierarchical structure of dependency between transition and physical risks. The main hypothesis is that, in a given scenario, physical risk influences in the same way all the companies, independently from their responsiveness to transition risk. In other words, we first consider the impact of a low and high climate physical risk on green, brown and neutral companies. Then we assume that, given a predetermined level of physical risk (low or high), green, brown and neutral firms perform differently, according to their exposure to transition risk.

We will focus on the disorderly transition, the hot house world and the orderly transition scenarios. The set of underlying assumptions that defines each scenario is denoted as $\mathcal{C}_{dis}, \mathcal{C}_{hhw}, \mathcal{C}_{ord}$, respectively. In order to associate probability to each scenario, let $\boldsymbol{R}$ be a vector of random variables representing financial returns and a physical risk index. Specifically, let R_g, R_b and R_n denote the returns of green, brown and neutral companies, respectively, and let R_p represent a suitable physical risk index, so that $\boldsymbol{R}' = [R_g, R_b, R_n, R_p]$. The joint distribution function of these variables is described by the *cumulative distribution function (CDF)* $F_{\boldsymbol{R}}(\boldsymbol{r}) : \mathbb{R}^4 \to [0, 1]$, which is defined as:

$$F_{\boldsymbol{R}}(\boldsymbol{r}) = Pr(R_g \leq r_g, R_b \leq r_b, R_n \leq r_n, R_p \leq r_p) \tag{1}$$

In disorderly-related scenarios, a proactive approach is addressed to keep global warming under control and policies are introduced with medium-high speed. In this context, green companies are likely to have an advantage relatively to brown companies, so that their stock returns would experience an increase whereas, in contrast, brown company stocks' returns would experience a decrease. On the other hand, physical risk index is assumed to remain stably low, under a pre-determined threshold. This narrative can be consistently translated into a climate scenario, *i.e.*:

$$\mathcal{C}_{dis} = \left\{ R_g \geq q_g^{\beta}, R_b \leq q_b^{\alpha};\ R_n, R_p \leq q_p^{\gamma} \right\} \tag{2}$$

where the β, α and γ quantiles of green and brown stock returns' distributions and physical index distribution are given by $Pr(R_g \geq q_g^{\beta}) = \beta$ (such that $Pr(R_g < q_g^{\beta}) = 1 - \beta$), $Pr(R_b \leq q_b^{\alpha}) = \alpha$ and $Pr(R_p \leq q_p^{\gamma}) = \gamma$, respectively. The probabilistic scenario associated to $\mathcal{C}_{dis}$ is described by the following joint probability:

$$\begin{aligned} Pr(\mathcal{C}_{dis}) &= Pr(R_g \geq q_g^{\beta},\ R_b \leq q_b^{\alpha};\ R_n, R_p \leq q_p^{\gamma}) = \\ \int_{-\infty}^{q_p^{\gamma}} \int_{-\infty}^{\infty} & Pr(R_g \geq q_g^{\beta},\ R_b \leq q_b^{\alpha} \mid R_n, R_p) f_{R_n|R_p}(r_n \mid r_p) f_{R_p}(r_p)\, dr_n\, dr_p \end{aligned} \tag{3}$$

In hot-house-world-related scenarios, current policies are preserved, emissions grow, and temperatures are expected to increase by more than 3.0°C in a 50-year period. In these scenarios, representing a low carbon transition risk in conjunction with high climate physical risks, brown companies are expected to increase in value, and green ones to do the opposite. To this narrative we associate the following climate scenario:

$$\mathcal{C}_{hhw} = \left\{ R_g \leq q_g^{\alpha}, R_b \geq q_b^{\beta};\ R_n, R_p \geq q_p^{\gamma} \right\} \tag{4}$$

where the α, β and γ quantiles of green and brown stock returns' distributions and physical index distribution are given by $Pr(R_g \leq q_g^{\alpha}) = \alpha$, $Pr(R_b \geq q_b^{\beta}) = \beta$ (such that $Pr(R_b < q_b^{\beta}) = 1 - \beta$) and $Pr(R_p \geq q_p^{\gamma}) = 1 - \gamma$, respectively. The probability associated to such scenarios can be computed as follows:

$$Pr(\mathcal{C}_{hhw}) = Pr(R_g \leq q_g^{\alpha},\ R_b \geq q_b^{\beta};\ R_n, R_p \geq q_p^{\gamma}) = \int_{q_p^{\gamma}}^{\infty} \int_{-\infty}^{\infty} Pr(R_g \leq q_g^{\alpha},\ R_b \geq q_b^{\beta} \mid R_n, R_p)\, f_{R_n|R_p}(r_n \mid r_p)\, f_{R_p}(r_p)\, dr_n\, dr_p \tag{5}$$

As far as orderly-related scenarios are concerned, policy constraints to meet climate transition goals are implemented smoothly, allowing firms to progressively adapt to the new business setting. Investors would expect, therefore, asset returns to move around their median values (*i.e.* with no abrupt price changes), while physical risk index is relative subdued. Such climate state can be described as:

$$\mathcal{C}_{ord} = \left\{ q_g^L \leq R_g \leq q_g^U, q_b^L \leq R_b \leq q_b^U;\ q_n^L \leq R_n \leq q_n^U, R_p \leq q_p^{\gamma} \right\} \tag{6}$$

where L and U represent the symmetric lower and upper percentile around the median quantile of the respective distributions. The probability associated to such climate state can be computed as follows:

$$\begin{aligned} Pr(\mathcal{C}_{ord}) &= Pr(q_g^L \leq R_g \leq q_g^U, q_b^L \leq R_b \leq q_b^U;\ q_n^L \leq R_n \leq q_n^U, R_p \leq q_p^{\gamma}) \\ &= \int_{-\infty}^{q_p^{\gamma}} \int_{-\infty}^{\infty} Pr(q_g^L \leq R_g \leq q_g^U, q_b^L \leq R_b \leq q_b^U | q_n^L \leq R_n \leq q_n^U, R_p \\ &\leq q_p^{\gamma}) f_{R_n|R_p}(r_n \mid r_p) f_{R_p}(r_p)\, dr_n\, dr_p \end{aligned} \tag{7}$$

In the current study, in line with the literature, α and β are set equal to 0.2. In the orderly transition scenario, for green, neutral and brown indexes, q_i^L and q_i^U (with $i = g, n, b$) are set to 0.40 and 0.60, respectively. Regarding the physical index, q_p^{γ} is the quantile associated to a value of the index equal to 1 in order to distinguish low and high physical risk. As a matter of fact, by construction, the index used for the physical risk reports values greater than the unitary threshold when an extreme weather event is occurred. The probability associated to a low physical risk (γ) is approximately equal to 0.9.

The underlying assumptions of each climate scenario are schematically illustrated below for clarity (See Table 1):

Table 1 Summary of underlying assumptions for each climate scenario

Climate hypothesis	p	g	n	b
Disorderly trans. ($\mathcal{C}_{dis}$)	$R_p \leq q_p^{\gamma}$	$R_g \geq q_g^{\beta}$	R_n	$R_b \leq q_b^{\alpha}$
Hot house world ($\mathcal{C}_{hhw}$)	$R_p \geq q_p^{\gamma}$	$R_g \leq q_g^{\alpha}$	R_n	$R_b \geq q_b^{\beta}$
Orderly trans. ($\mathcal{C}_{ord}$)	$R_p \leq q_p^{\gamma}$	$q_g^L \leq R_g \leq q_g^U$	$q_n^L \leq R_n \leq q_n^U$	$q_b^L \leq R_b \leq q_b^U$

For each row of the table a climate scenario is presented; columns report relevant climate variables, where p stands for "*physical*", g for "*green*", n for "*neutral*" and b for "*brown*". For each variable, climate scenarios are identified through the respective "portions" of the multivariate probability space

3 Measures of climate systemic risk

In order to identify potential vulnerabilities of the financial system in each scenario $\mathcal{C} \in \{\mathcal{C}_{dis}, \mathcal{C}_{hhw}, \mathcal{C}_{ord}\}$, we compute, for each bank, four metrics. The first three are strictly related to each other and they are the conditional expected return (*C-ER*), the conditional value-at-risk (*C-VAR*), the conditional expected shortfall (*C-ES*). Finally, based on *C-ER*, we quantify the conditional capital at risk (*CRISK*) of the financial institutions in each climate scenario.

Let R_i be a random variable denoting the stock return of bank i. The $C\text{-}ER_i^{\mathcal{C}}$ can be computed as:

$$E(R_i|\mathcal{C}) = \frac{\int_{-\infty}^{\infty} r_i \cdot f_{\mathcal{C}|R_i}(\mathcal{C}|r_i) \cdot f_{R_i}(r_i)\, dr_i}{\int_{-\infty}^{\infty} f_{\mathcal{C}|R_i}(\mathcal{C}|r_i) \cdot f_{R_i}(r_i)\, dr_i}, \quad \mathcal{C} \in \{\mathcal{C}_{dis}, \mathcal{C}_{hhw}, \mathcal{C}_{ord}\} \tag{8}$$

where $f(\mathcal{C}|r_i) \cdot f(r_i)$ represents the joint density function of r_i and $\mathcal{C}$, whereas the denominator $\int_{-\infty}^{\infty} f(\mathcal{C}|r_i) \cdot f(r_i)\, dr_i$ represents the probability of occurrence of climate scenario $Pr(\mathcal{C})$. Ultimately, the computation of C-ER of bank i under the climate scenario $\mathcal{C}$ reduces to:

$$E(R_i|\mathcal{C}) = \int_{-\infty}^{\infty} r_i \frac{f_{\boldsymbol{R}}(r_i,\ \mathcal{C})}{Pr(\mathcal{C})}\, dr_i, \quad \mathcal{C} \in \{\mathcal{C}_{dis}, \mathcal{C}_{hhw}, \mathcal{C}_{ord}\} \tag{9}$$

Concerning the $C\text{-}VAR_i^{\mathcal{C}}$, this represents the quantile of stock i's distribution (conditional on the climate state $\mathcal{C}$) that solves the following equation:

$$Pr(R_i \leq VaR_\delta^i|\mathcal{C}) = \delta, \quad \mathcal{C} \in \{\mathcal{C}_{dis}, \mathcal{C}_{hhw}, \mathcal{C}_{ord}\} \tag{10}$$

that is the quantile of the distribution (conditional on the climate state $\mathcal{C}$) which leaves at its left a probability equal to δ. Formally:

$$F(VaR_\delta^i|\mathcal{C}) = \frac{\int_{-\infty}^{VaR_\delta^i} f(\mathcal{C}|r_i) \cdot f(r_i)\, dr_i}{\int_{-\infty}^{\infty} f(\mathcal{C}|r_i) \cdot f(r_i)\, dr_i} = \delta, \quad \mathcal{C} \in \{\mathcal{C}_{dis}, \mathcal{C}_{hhw}, \mathcal{C}_{ord}\} \tag{11}$$

where $f(\mathcal{C}|r_i) \cdot f(r_i)$ represents the joint density function of r_i and $\mathcal{C}$, whereas the denominator $\int_{-\infty}^{\infty} f(\mathcal{C}|r_i) \cdot f(r_i)\, dr_i$ represents the probability of occurrence of climate scenario $\mathcal{C}$, i.e. $Pr(\mathcal{C})$. By replacing $f(\mathcal{C}|r_i) \cdot f(r_i)$ and $\mathcal{C}$, we obtain:

$$F(VaR_\delta^i|\mathcal{C}) = \int_{-\infty}^{VaR_\delta^i} \frac{f_{\boldsymbol{R}}(r_i,\ \mathcal{C})}{Pr(\mathcal{C})}\, dr_i = \delta, \quad \mathcal{C} \in \{\mathcal{C}_{dis}, \mathcal{C}_{hhw}, \mathcal{C}_{ord}\} \tag{12}$$

Finally, the $C\text{-}ES_i^{\mathcal{C}}$ is defined as the average return r of bank i below (*i.e.* to the left of) the VaR_δ^i under the climate scenario $\mathcal{C}$, so that:

$$C\text{-}ES_\delta^i = E(R_i|R_i \leq VaR_\delta^i, \mathcal{C}) = \int_{-\infty}^{VaR_\delta^i} r_i \cdot \frac{f_{\boldsymbol{R}}(r_i,\ \mathcal{C})}{Pr(r_i \leq VaR_\delta^i|\ \mathcal{C})}\, dr_i, \quad \mathcal{C} \in \{\mathcal{C}_{dis}, \mathcal{C}_{hhw}, \mathcal{C}_{ord}\} \tag{13}$$

In the present study, in line with the previous literature, in order to compute $C\text{-}VAR_i^{\mathcal{C}}$ and $C\text{-}ES_i^{\mathcal{C}}$, we set δ equal to 0.1.

Concerning the *CRISK*, the methodology is derived from Jung et al. (2021), who extended the *SRISK* measure of Brownlees and Engle (2017) and Acharya et al. (2012), which denotes the capital shortfall of a firm conditional on a systemic event. Following the original notation

used in Brownlees and Engle (2017), we start by computing the capital shortfall (CS) of bank i at time t, which is defined as:

$$CS_{i,t} = k \cdot A_{i,t} - W_{i,t} = k(D_{i,t} + W_{i,t}) - W_{i,t} = k \cdot D_{i,t} - (1-k) \cdot W_{i,t} \tag{14}$$

where $A_{i,t}$ is the value of *quasi* assets of bank i at time t[4], $W_{i,t}$ and $D_{i,t}$ are the observed market capitalization and debt of bank i at time t, respectively, and k is a scalar denoting the prudential capital fraction set by the regulator.

Given the linearity property of the expected value operator $E(\bullet)$, the expected value of CS of bank i at time t conditional on a climate event can be computed as[5]:

$$\begin{aligned} C\text{-}CS^{\mathcal{C}}_{i,t} = E_t(CS_{i,t+h}|\mathcal{C}) = E_t(k \cdot D_{i,t+h} - (1-k) \cdot W_{i,t+h}|\mathcal{C}) = \\ k \cdot E_t(D_{i,t+h}|\mathcal{C}) - (1-k)E_t(W_{i,t+h}|\mathcal{C}) \end{aligned} \tag{15}$$

with $\mathcal{C} \in \{\mathcal{C}_{dis}, \mathcal{C}_{hhw}, \mathcal{C}_{ord}\}$. Moreover, it is reasonable to treat the total debt D_i as a constant (*i.e.* $E_t(D_{i,t+h}|r_{m,t+h} < \psi) = D_{i,t}$), under the assumption that, in case of systemic events, the debt cannot be renegotiated. That is:

$$C\text{-}CS^{\mathcal{C}}_{i,t} = k \cdot D_{i,t} - (1-k) \underbrace{E_t(W_{i,t+h}|\mathcal{C})}_{W_{i,t}(1+LR\ C\text{-}ER^{\mathcal{C}}_{i,t})} \tag{16}$$

with $\mathcal{C} \in \{\mathcal{C}_{dis}, \mathcal{C}_{hhw}, \mathcal{C}_{ord}\}$. A central role is played by the factor $E_t(W_{i,t+h}|R_{crf,t+h} < \psi)$, which represents the expected value of bank's capitalization conditional on a climate systemic event. This factor can also be restated as $W_{i,t}(1+LR\ C\text{-}ER^{\mathcal{C}}_{i,t})$, where $LR\ C\text{-}ER^{\mathcal{C}}_{i,t}$ represents the Long Run $C\text{-}ER$ of bank i at time t under the climate scenario $\mathcal{C}$, that is:

$$LR\ C\text{-}ER^{\mathcal{C}}_{i,t} = e^{C\text{-}ER^{\mathcal{C}}_{i,t}} - 1 \tag{17}$$

with $C\text{-}ER^{\mathcal{C}}_{i,t}$ indicating the annualized conditional expected return of bank i's stock at time t[6] under the climate setting $\mathcal{C} = \mathcal{C}_{dis}, \mathcal{C}_{hhw}, \mathcal{C}_{ord}$. In practice, the $LR\ C\text{-}ER^{\mathcal{C}}_{i,t}$ represents the one-year-ahead expected return assuming a specific climate stress scenario. Starting from $LR\ C\text{-}ER^{\mathcal{C}}_{i,t}$, the climate risk propagates through the $C\text{-}CS$: in particular, a lower $LR\ C\text{-}ER^{\mathcal{C}}_{i,t}$ corresponds to a higher climate risk exposure and, as a consequence, to a higher $C\text{-}CS$. Clearly, this is not a warning sign *per se*, since the $C\text{-}CS$ will remain negative if the bank is adequately capitalized.

In its standard formulation, the $CRISK^{\mathcal{C}}_{i,t}$ quantifies the capital at risk for each bank i at time t under a specific climate scenario as:

$$CRISK^{\mathcal{C}}_{i,t} = \max(0,\ C\text{-}CS^{\mathcal{C}}_{i,t}) \tag{18}$$

since the capital shortfall $CS_{i,t}$ has economic relevance only when is greater than 0, *i.e.* when market capitalization of bank i at time t ($W_{i,t}$) is lower than the regulatory capital requirement ($k \cdot A_{i,t}$). Individual results for $CRISK$ are not reported for brevity. Despite differences in exposure to climate risk could emerge on an individual basis, here we are interested in quantifying the climate systemic risk and identify potential criticality at a country and

[4] Here we refer to $A_{i,t}$ as *quasi* assets since they are computed by using the market capitalization $W_{i,t}$ instead of the book value of equity.

[5] The linearity property of $E(\bullet)$ states that for any two random variables X and Y, and any two constants a and b, the following holds: $E(aX + bY) = aE(X) + bE(Y)$.

[6] Specifically, we multiplied $C\text{-}ER^{\mathcal{C}}_{i,t}$ by 52.

European level. For each climate scenario $\mathcal{C}$, the systemic CRISK, aggregated on a country level, has been determined as:

$$CRISK^{\mathcal{C}}_{c,t} = \sum_{i_c=1}^{N} CRISK^{\mathcal{C}}_{i_c,t} \tag{19}$$

where i_c represents the bank i in country c and $\mathcal{C}$ the specific climate setting, with $\mathcal{C} \in \{\mathcal{C}_{dis}, \mathcal{C}_{hhw}, \mathcal{C}_{ord}\}$.

4 Data

4.1 Climate risk variables

Climate risks (transition and physical) have been measured through the construction of suitable indexes. More specifically, the transition risk derives from the interaction between green, neutral and brown companies, since they are expected to perform differently according to the climate scenario one is assuming. On the other hand, physical risk index has been elaborated taking into account data provided by specialized data centers which monitor extreme weather events.

Green, neutral and brown companies. For each non-financial constituent of the STOXX Europe 600 index, we gathered from Bloomberg data about scope 1 and scope 2 annual GHG emission[7] for the decade between 2014 and 2023[8].

Non-financial companies have been then categorized into quintiles, in such a way that they are classified as green or brown when included in the first and fifth GHG quintiles, respectively, and as neutral otherwise. For each group, we then constructed 3 indexes, by computing the cross-sectional median of weekly returns, denoted as $\bar{r}_{g,t}$, $\bar{r}_{b,t}$, $\bar{r}_{n,t}$, respectively, over the time horizon t going from 1 to T. The distinctive feature of green, neutral, and brown firms is their vulnerability to transition to a low-carbon economy, with green (brown) firms exhibiting the lowest (highest) risk exposure, and neutral firms having average risk exposure. The inter-dependence between green, neutral, and brown returns determines the systemic impact of different climate scenarios.

Main statistics of green, neutral, brown indexes are synthesized in Table 2.

Green, neutral and brown indexes result to be strongly positive correlated[9]. The presence of high kurtosis (around 12.0 for all the indexes) and negative skewness confirm an evident

[7] To help delineate direct and indirect emission sources, the GHG *Protocol Corporate Standard* has defined three scopes for GHG accounting and reporting purposes. For our purposes, we limit our analysis to the first two, since the third one is an optional reporting category which allows for the treatment of all other indirect emissions. Scope 1 includes direct GHG emissions, occurring from sources that are owned or controlled directly by a company. Scope 2 accounts for GHG emissions from the generation of purchased electricity consumed by a company. Purchased electricity is defined as electricity that is purchased or otherwise brought into the organizational boundary of a company.

[8] We rely on absolute GHG emissions as our baseline measure since they provide a direct indication of the aggregate decarbonisation process associated with each firm and are consistent with the transition-risk mechanisms embedded in NGFS scenarios. We are aware that alternative standardizations (e.g., GHG scaled by enterprise value, revenues, or total assets) could lead to different ranking based on carbon intensity. However, their cross-sectional rank correlations with absolute emissions remain high, and our main empirical results are mainly unchanged. For this reason, and to remain consistent with the NGFS framework, we retain absolute emissions as our preferred specification.

[9] Specifically, correlation between green and neutral is about 0.96, between green and brown is approximately equal to 0.86 and, finally, between neutral and brown about 0.94.

Table 2 Summary statistics of green, neutral and brown indexes

Climate indexes	Min	Mean	Median	Max	Std dev	Skewness	Kurtosis	Obs.
Green	−0.1861	0.0023	0.0046	0.1146	0.0244	−1.0727	12.3141	522
Neutral	−0.1791	0.0016	0.0042	0.0919	0.0226	−1.2669	12.4485	522
Brown	−0.2032	0.0009	0.0024	0.1102	0.0253	−1.2214	12.5478	522

This table reports summary statistics of green, neutral and brown indexes. All indexes are negatively skewed, indicating a higher probability of extreme negative returns than positive ones and exhibit significant kurtosis, particularly the brown portfolio, indicating fat tails and a higher likelihood of extreme returns

departure from normality distribution assumptions. All three indexes have a positive mean, albeit small, suggesting a positive average return over the sample period. From summary statistics, reported in Table 2, it is evident that green firms outperform brown ones both in terms of mean returns (0.23% vs 0.09%) and in terms of volatility (2.4% vs 2.5%). Starting from 2017, green index has been strongly overperforming compared to neutral and brown index. This pattern may be interpreted as the realization of a disorderly transition scenario, in which abrupt policy interventions, technological shifts, or changes in investor sentiment disproportionately benefit low-emission firms while penalizing carbon-intensive companies. Under the 2015 Paris agreement, 196 countries pledged to limit global warming to well below 2.0°C, and ideally not more than 1.5°C above preindustrial levels. That target, if pursued, would manifest in decarbonization across industries, creating major shifts in commodity demand for the energy and mining industries and likely resulting in declining global revenue pools.

As more countries adopt policies and regulations to reduce emissions and promote clean energy, the demand for fossil fuels and other high-emitting assets may decline, potentially causing these assets to become stranded and lose value. In light of this, financial institutions who adopted an expansive investment policy in favor of green activities are supposed to pursue a concrete benefit in terms of extra returns, whereas those with portfolios heavily concentrated in carbon-intensive sectors are likely to face relative underperformance and increasing transition risk exposures.

Physical Risk Index. To proxy physical risk, we rely on the European Extreme Events Climate Index (E^3CI) published on the website https://climateindex.eu/ and updated with monthly frequency. The project is born from the collaboration between the *International Foundation Big Data and Artificial Intelligence for Human Development* (IFAB), the Italian foundation *Centro Euro-Mediterraneo sui Cambiamenti Climatici* (CMCC Foundation) and a private entity (Leithà), which acts as a research center promoted by Unipol Group within the big data and computer science sector.

E^3CI exploits atmospheric reanalysis ERA5, which covers global climate in the period from January 1940 to present. More specifically, E^3CI is based on the re-elaboration, at country level, of 7 weather indicators (maximum and minimum temperatures, droughts, precipitations, winds, hails and forest fires). Each timeseries is then standardized with respect a reference period typically longer than one century, such that occurrences above 1.0 (unitary threshold) represent extreme weather events. For each European country, E^3CI is eventually computed as the arithmetic mean of the 7 weighted standardized weather indicators. For a more exhaustive description of the E^3CI construction, please refer to the technical notes reported on the website https://climateindex.eu/.

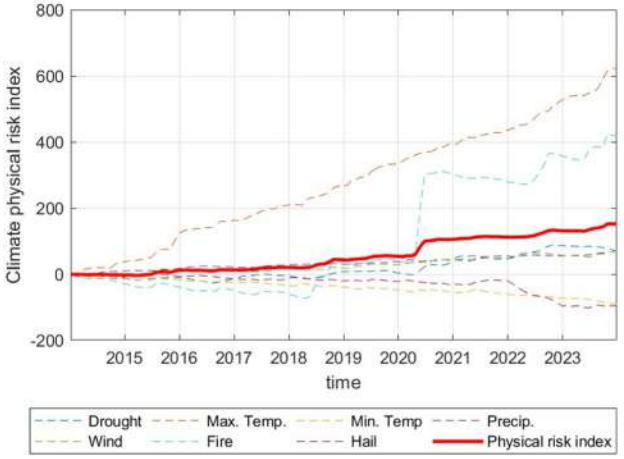

Fig. 2 European climate physical risk index. This figure shows the cumulated 7 European physical risk indicators starting from 2014 (maximum and minimum temperatures, droughts, precipitations, winds, hails and forest fires). Each risk index has been constructed as the weighted average of the country-specific indicators, using as weights their respective gross domestic products. When needed, GDPs have been previously converted in EUR. The solid red line represents the cumulated European physical risk index; it has been computed as the arithmetic mean of the 7 European risk indicators. A determinant role is played by the constant rising of maximum temperatures

In order to come to an aggregated European physical risk index, we examined the 7 indexes aforementioned for 37 European countries[10]. Then, for each of the 7 indicators, from 2014 to 2023, we computed the weighted average, using as weights the gross domestic product of the respective countries. The E^3CI at European level has been constructed as the arithmetic mean of the 7 weighted indicators (Fig. 2).

4.2 Sample of financial institutions

The sample of European financial institutions is composed by 43 banks. From Bloomberg database, we downloaded weekly time series of ordinary stock prices, adjusted for dividend and stock splits. Time series cover a decade period, from January 1, 2014 to December 31, 2023. Stock prices have been converted into stock returns by computing the weekly percentage variation ($r_{i,t} = \frac{p_{i,t}}{p_{i,t-1}} - 1$). Summary statistics of bank stocks' returns are synthesized in Table 3.

The overall market capitalization of the sample is about EUR 1.100bn by the end of 2023[11].

[10] The 37 European countries are: 1) Belgium; 2) Bulgaria; 3) Czechia; 4) Denmark; 5) Germany; 6) Estonia; 7) Ireland; 8) Greece; 9) Spain; 10) France; 11) Croatia; 12) Italy; 13) Cyprus; 14) Latvia; 15) Lithuania; 16) Luxembourg; 17) Hungary; 18) Malta; 19) Netherlands; 20) Austria; 21) Poland; 22) Portugal; 23) Romania; 24) Slovenia; 25) Slovakia; 26) Finland; 27) Sweden; 28) Iceland; 29) Norway; 30) Switzerland; 31) United Kingdom; 32) Bosnia and Herzegovina; 33) Montenegro; 34) North Macedonia; 35) Albania; 36) Serbia; 37) Turkey.

[11] The most represented banks in term of capitalization are as follows: HSBC Holdings (EUR 141.2 bn), UBS Group (EUR 97.3 bn), BNP Paribas (EUR 71.8 bn), Banco Santander (EUR 61.2 bn), Intesa Sanpaolo (EUR 48.3 bn), Banco Bilbao Vizcaya Argentaria (EUR 48.0 bn), ING Group (EUR 47.3 bn) and Unicredit (EUR 43.8 bn), Nordea Bank (EUR 39.6 bn) and Credit Agricole (EUR 39.2 bn).

Table 3 Summary statistics of bank stocks' returns

No.	Bank name	Min	Mean	Median	Max	Std. dev.	Skewness	Kurtosis	Obs.
1	Credit Agricole SA	−0.2620	0.0017	0.0025	0.1626	0.0464	−0.3510	6.0723	522
2	BNP Paribas SA	−0.1773	0.0012	0.0020	0.2127	0.0457	−0.1030	5.7319	522
3	Societe Generale SA	−0.2688	0.0004	0.0024	0.2733	0.0535	−0.2547	6.4174	522
4	Banco Santander SA	−0.2585	0.0003	−0.0002	0.3352	0.0492	0.5175	9.4846	522
5	Banco Bilbao Vizcaya Argentaria SA	−0.2449	0.0009	0.0011	0.2767	0.0472	0.3653	8.4637	522
6	ING Groep NV	−0.3156	0.0017	0.0005	0.2280	0.0476	−0.4066	9.1012	522
7	UniCredit SpA	−0.2846	0.0015	0.0026	0.1996	0.0580	−0.1927	4.8321	522
8	Intesa Sanpaolo SpA	−0.2346	0.0018	0.0038	0.1420	0.0450	−0.4992	5.8010	522
9	Commerzbank AG	−0.2679	0.0017	−0.0004	0.2645	0.0603	0.0274	5.1195	522
10	Deutsche Bank AG	−0.2466	−0.0001	−0.0003	0.2434	0.0555	0.0632	5.0575	522
11	DNB Bank ASA	−0.2475	0.0016	0.0021	0.1650	0.0406	−0.4208	6.5142	522
12	Danske Bank A/S	−0.2372	0.0015	0.0015	0.2031	0.0383	−0.2443	7.6600	522
13	Erste Group Bank AG	−0.2230	0.0019	0.0020	0.2563	0.0486	−0.0021	7.6062	522
14	KBC Group NV	−0.2228	0.0016	0.0019	0.2735	0.0424	−0.0188	8.5121	522
15	Swedbank AB	−0.2497	0.0006	0.0021	0.1172	0.0395	−1.0437	8.5497	522
16	Raiffeisen Bank International AG	−0.3177	0.0011	0.0011	0.3109	0.0574	−0.2579	8.3182	522
17	Banco BPM SpA	−0.2383	0.0013	0.0029	0.2829	0.0674	−0.0173	4.7431	522
18	Mediobanca Banca di Credito Finanziario SpA	−0.2854	0.0022	0.0047	0.2180	0.0474	−0.3890	7.1311	522
19	BPER Banca SPA	−0.2394	0.0012	0.0012	0.2231	0.0605	0.0431	4.1265	522
20	Jyske Bank A/S	−0.1710	0.0018	0.0012	0.1588	0.0397	−0.1971	5.2781	522
21	Powszechna Kasa Oszczednosci Bank Polski SA	−0.2463	0.0014	0.0014	0.2023	0.0448	−0.1305	6.0323	522
22	Bank Polska Kasa Opieki SA	−0.3026	0.0007	0.0004	0.2225	0.0466	−0.6341	8.9445	522

Table 3 continued

No.	Bank name	Min	Mean	Median	Max	Std. dev.	Skewness	Kurtosis	Obs.
23	Banca Popolare di Sondrio SPA	−0.2486	0.0023	0.0029	0.1910	0.0510	−0.0843	5.9604	522
24	Bank of Ireland Group PLC	−0.2474	0.0018	0.0000	0.2125	0.0579	−0.1399	4.7568	522
25	Banco Comercial Portugues SA	−0.2501	−0.0008	0.0000	0.3101	0.0669	0.1447	4.5837	522
26	Skandinaviska Enskilda Banken AB	−0.2445	0.0013	0.0036	0.1964	0.0382	−0.6418	7.7505	522
27	Sydbank AS	−0.2206	0.0022	0.0034	0.1548	0.0407	−0.2787	6.3103	522
28	Banca Monte dei Paschi di Siena SpA	−0.6859	−0.0103	−0.0053	0.5800	0.0927	−0.5533	15.1255	522
29	CaixaBank SA	−0.1727	0.0011	0.0010	0.2704	0.0470	0.4776	6.0158	522
30	AIB Group PLC	−0.4595	−0.0006	0.0000	0.4041	0.0777	−0.1155	9.7228	522
31	Ringkjoebing Landbobank A/S	−0.1837	0.0033	0.0032	0.1370	0.0298	−0.4000	7.2898	522
32	Santander Bank Polska SA	−0.2737	0.0016	0.0016	0.2041	0.0492	−0.0416	5.8772	522
33	HSBC Holdings PLC	−0.1372	0.0004	0.0010	0.1564	0.0339	0.1651	4.8930	522
34	Barclays PLC	−0.2425	0.0001	0.0003	0.2213	0.0498	−0.0014	6.0927	522
35	NatWest Group PLC	−0.1999	0.0003	0.0021	0.2595	0.0525	0.1055	5.8151	522
36	Bankinter SA	−0.2175	0.0018	0.0021	0.2555	0.0439	0.1626	7.0664	522
37	Standard Chartered PLC	−0.1854	−0.0002	0.0008	0.2758	0.0483	0.2653	6.3979	522
38	Banco de Sabadell SA	−0.2709	0.0012	0.0036	0.3326	0.0626	0.3363	6.3193	522
39	Lloyds Banking Group PLC	−0.1964	−0.0000	−0.0015	0.2780	0.0453	0.4742	8.7041	522
40	Nordea Bank Abp	−0.2675	0.0010	0.0028	0.1508	0.0377	−0.6758	8.9195	522
41	Svenska Handelsbanken AB	−0.1901	0.0004	−0.0005	0.1701	0.0364	−0.1437	5.5262	522
42	Banque Cantonale Vaudoise	−0.0725	0.0023	0.0027	0.1700	0.0230	0.6263	8.4218	522
43	UBS Group AG	−0.1814	0.0021	0.0023	0.1808	0.0393	−0.1568	5.5462	522

Note: Stocks' returns are computed as the first difference in weekly prices. Ordinary (common) shares are selected. Each bank has 522 weekly observations from 1 January 2014 to 31 December 2023. Most stocks show left skewness and high kurtosis

Preliminarly, we tested banks' exposure to green, neutral and brown indexes (controlling for the STOXX Europe 600), by performing, for each institution, an OLS regression with the following specification:

$$r_{i,t} = \alpha_i + \mathbf{x_t'}\boldsymbol{\beta_i} + \epsilon_{i,t} \tag{20}$$

where $\mathbf{x_t'}$ is a vector containing green, brown, neutral index, as well the EURO STOXX 600 index as controlling variable. Results are reported in Appendix B. T-stats reported in the table have been computed by bootstrapping residuals 10.000 times. From the analysis conducted, it emerges that European financial institutions are heavily exposed to brown companies, with an average β_{brown} equal to 1.53. On the other hand, exposure to green and neutral appears to be low and not always statistically significant. If regulatory interventions will be implemented to shift into less carbon-intensive economy to meet the Paris agreement goal, the returns of "brown" companies are likely to fade rapidly. As a consequence, in the absence of corrective adjustments in portfolio composition, bank stock returns would be expected to decrease correspondingly, with their trajectory falling significantly below that of the STOXX Europe 600 index over the short/medium term.

5 Climate scenarios' construction

Once climate risk variables have been defined, we have assumed a hierarchical structure of dependence between them. Extending the methodology adopted by Ojea-Ferreiro et al. (2024), the dependency structure of the set of climate variables (*i.e.* the climate physical risk index, returns of green, neutral and brown companies) has been modeled with the PCC method through a C-vine copula, which allows us to decompose a n joint density function $h(x_1, x_2, ..., x_n)$ into $\frac{n\cdot(n-1)}{2}$ appropriate pair-copulas and n marginal density functions. Vine copulas have been used in several financial modeling applications, such as the estimation of portfolio risk (Allen et al., 2013), portfolio optimization in energy markets (Allevi et al., 2019), and the study of the interdependence of companies sustainability scores (Czado et al., 2022).

Since we deal with copulas, which require uniform marginal distributions, we transformed original variables accordingly. Regarding standardized residuals of banks' returns, green, neutral and brown indexes, we obtained a time series of pseudo observations by evaluating the cumulative function of the Hansen's *skew-t* distribution, thereby transforming the original data into the unit interval [0, 1]. As far as the physical risk index is concerned, we transformed the original variable through a non-parametric procedure, *i.e.* by computing its empirical cumulative distribution. From now on, we follow the standard notation which conventionally denotes with the letter u the transformed variables.

The structure of dependence between the climate physical risk index (u_p) and green (u_g), neutral (u_n) and brown (u_b) companies is compactly and effectively summarized by the following upper triangular matrix $\mathbf{V}$:

$$\begin{bmatrix} 1 & 1 & 1 & 1 \\ 0 & 2 & 2 & 3 \\ 0 & 0 & 3 & 2 \\ 0 & 0 & 0 & 4 \end{bmatrix} \tag{21}$$

where each number corresponds to a different index. In particular, physical risk index (u_p) is associated to number 1, whereas green (u_g), neutral (u_n) and brown (u_b) indexes are associated to number 2, 3 and 4, respectively. Each tree of the vine copula is described by

the corresponding row of the matrix in conjunction with the leading diagonal $diag(\mathbf{V})$. The C-vine is composed of three trees having the physical risk as the central node connected to green, neutral and brown marginal distributions through the copulas $C(u_p, u_g)$, $C(u_p, u_n)$ and $C(u_p, u_b)$ respectively. The choice of physical risk index as a central node relies on the evidence that extreme weather events and long-term climate changes are systemic drivers of financial and operational impacts.

More specifically, the first tree of the vine copula is associated to the first row and the leading diagonal of the matrix. Therefore, to the pair of numbers (1,2), *i.e.* the second number on the first row and on the leading diagonal, is associated the copula $C(u_p, u_g)$, to the pair of numbers (1,3), *i.e.* the third number on the first row and on the leading diagonal, is associated the copula $C(u_p, u_n)$ and, finally, to the pair of numbers (1,4), *i.e.* the fourth number on the first row and on the leading diagonal, is associated the copula $C(u_p, u_b)$.

The second tree of the vine copula is represented by the second row and the leading diagonal, with the elements in the first row now containing the respective conditioning variables. Therefore, to the 3-tuple of numbers (1,2,3), *i.e.* the third number on the first two rows and on the leading diagonal, is associated the conditional copula $C(u_g, u_n|u_p)$, and to the 3-tuple of numbers (1,3,4), *i.e.* the fourth number on the first two rows and on the leading diagonal, is associated the conditional copula $C(u_b, u_n|u_p)$. This approach involves the computation of the marginal conditional distributions $F_{j|p}(u_j|u_p)$, with $j = g, n, b$. It can be shown that they can be computed as:

$$F_{j|p}(u_j|u_p) = \frac{\partial C(u_j, u_p)}{\partial u_p} = h(u_j, u_p, \boldsymbol{\Theta}) \text{ with } j = g, n, b \tag{22}$$

where $h(\cdot, \cdot, \boldsymbol{\Theta})$ represents the so-called $h\text{-}function$, with the second parameter corresponding to the conditioning variable, and $\boldsymbol{\Theta}$ denoting the set of parameters for the copula of the joint distribution function of u_j and x_p. Appendix D provides a detailed overview of the set of parameters $\boldsymbol{\Theta}$ characterizing each of the bivariate copulas considered in the analysis[12].

Finally, the third tree of the vine copula is represented by the third row and the leading diagonal, with the elements in the first two rows now containing the respective conditioning variables. Therefore, to the 4-tuple of numbers (1, 3, 2, 4), *i.e.* the fourth number on the first three rows and on the leading diagonal, is associated the conditional copula $C(u_g, u_b|u_p, u_n)$. Appendix C provides a graphical representation of the structure of the implemented C-vine copula.

An illuminating perspective on the computational problem is provided by the 2D graphical representation of the copulas reported in Figures 3-5. As a matter of fact, copulas allow us to translate climate scenarios into portions of the probability space. Starting from four variables (physical risk index, and returns of green, neutral, and brown assets), we reduce the complexity of the probability space by focusing on conditional distributions instead of marginals, thereby *flattening* the problem into a dual-dimensional framework (green and brown assets only). In other words, here we are assuming that the impact of physical risk and neutral assets over green and brown ones has already been analyzed and properly taken into account. By adopting this approach, copulas assume a far more intuitive meaning, since they can be treated as addition and subtraction of portions of the probability space.

[12] The set $\boldsymbol{\Theta}$ includes one or more parameters, depending on the type of copula. For instance, the Gaussian copula involves the linear correlation ρ. The Student's t copula includes both the linear correlation ρ and the degrees of freedom η, which controls tails thickness and tail dependence. Archimedean copulas (such as the Gumbel, Clayton and Frank copulas) involves a dependence parameter, often denoted with θ, that governs the strength and asymmetry of dependence.

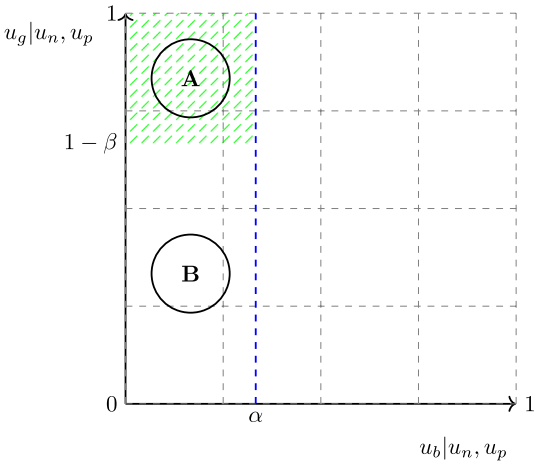

Fig. 3 2D Probability Space for the Climate Disorderly Transition Scenario

In the disorderly transition scenario $\mathcal{C}_{dis}$, we are assuming that $Pr(R_g \geq q_g^{\beta}; R_n) = 1-\beta$ (such that $Pr(R_g < q_g^{\beta}; R_n) = \beta$) and that $Pr(R_b \leq q_b^{\alpha}; R_n) = \alpha$, given a low level of physical risk, *i.e.* $Pr(R_p \leq q_p^{\gamma}) = \gamma$.

In terms of copulas, the joint probability associated to this scenario can be computed as follows:

$$\begin{aligned} Pr(\mathcal{C}_{dis}) &= Pr\left(R_g \geq q_g^{\beta}, R_b \leq q_b^{\alpha}; R_n \middle| R_p \leq 1\right) \\ &= \int_0^1 \int_0^{F_{R_p}(1)} C(u_g \geq 1-\beta, u_b \leq \alpha; u_n \middle| u_p)\, du_p\, du_n \end{aligned} \tag{23}$$

where

$$C((u_g \geq 1-\beta, u_b \leq \alpha|u_n)\big|u_p) = \overbrace{C_{b|p,n}(C_{b|p}(\alpha|u_p)|C_{n|p}(u_n|u_p)) - \underbrace{C_{g,b|p,n}(C_{g|p,n}(C_{g|p}(1-\beta|u_p)|C_{n|p}(u_n|u_p), C_{b|p,n}(C_{b|p}(\alpha|u_p)|C_{n|p}(u_n|u_p)))}_{\text{B}}}^{\text{(A+B)}} \tag{24}$$

In Fig. 3, x and y-axis report the conditional distribution of brown and green assets, given neutral ones and physical risk index, respectively. Graphically, our area of interest is colored in green and denoted with the letter A. Trivially, determining this area consists in computing the difference between the sum of areas $(A + B)$ and B.

In the hot house world scenario $\mathcal{C}_{hhw}$, we are assuming that $Pr(R_g \leq q_g^{\alpha}) = \alpha$ and that $Pr(R_b \geq q_b^{\beta}) = \beta$ (such that $Pr(R_b < q_b^{\beta}) = 1-\beta$), given a high level of physical risk, *i.e.* $Pr(R_p \geq q_p^{\gamma}) = 1-\gamma$. Similarly to the disorderly transition scenario, this probability can be computed as:

$$\begin{aligned} Pr(\mathcal{C}_{hhw}) &= Pr\left(R_g \leq q_g^{\alpha}, R_b \geq q_b^{\beta}; R_n, R_p \geq 1\right) \\ &= \int_0^1 \int_{F_{R_p}(1)}^1 C(u_g \leq \alpha, u_b \geq 1-\beta; u_n \middle| u_p)\, du_p\, du_n \end{aligned} \tag{25}$$

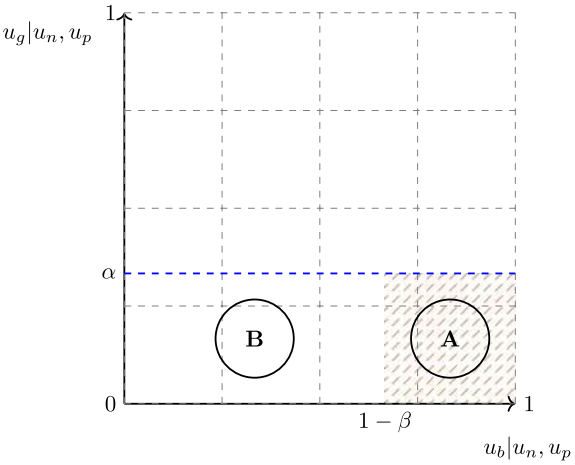

Fig. 4 2D Probability Space for the Climate Hot House World Scenario

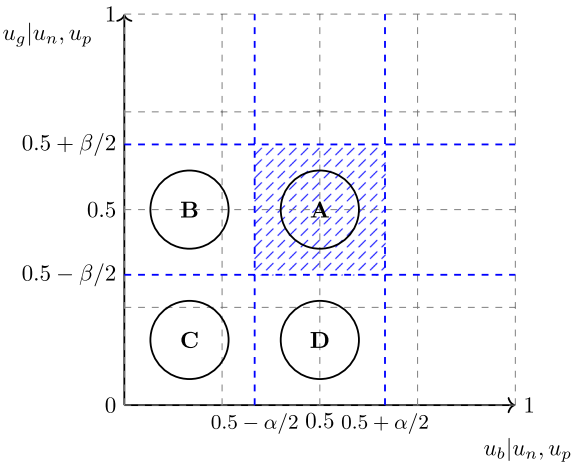

Fig. 5 2D Probability Space for the Climate Orderly Transition Scenario

where

$$C((u_g \leq \alpha, u_b \geq 1-\beta|u_n)|u_p) = \overbrace{C_{g|p,n}(C_{g|p}(\alpha|u_p)|C_{n|p}(u_n|u_p)) - C_{g,b|p,n}(C_{g|p,n}(C_{g|p}(\alpha|u_p)|C_{n|p}(u_n|u_p), C_{b|p,n}(C_{b|p}(1-\beta|u_p)|C_{n|p}(u_n|u_p)))}^{\text{(A+B)}} \underbrace{}_{\text{B}} \tag{26}$$

In Fig. 4, x and y-axis report the conditional distribution of brown and green assets, given neutral ones and physical risk index, respectively. Graphically, our area of interest is colored in brown and denoted with the letter A. As already specified for the disorderly transition scenario, determining the probability associated to the hot house world consists in computing the difference between the sum of areas $(A + B)$ and B.

Finally, in the orderly transition scenario $\mathcal{C}_{ord}$, we assume that $Pr(q_g^L \leq R_g \leq q_g^U)$, $Pr(q_b^L \leq R_b \leq q_b^U)$, $Pr(q_n^L \leq R_n \leq q_n^U)$, given a low level of physical risk, *i.e.* $Pr(R_p \leq q_p^\gamma)$. This can be restated in terms of copulas as:

$$Pr(\mathcal{C}_{ord}) = Pr(q_g^L \leq R_g \leq q_g^U, q_b^L \leq R_b \leq q_b^U; q_n^L \leq R_n \leq q_n^U, R_p \leq q_p^\gamma) = \int_e^f \int_0^{F_{R_p}(1)} C(a \leq u_g \leq b, c \leq u_b \leq d; u_n | u_p)\, du_p\, du_n \tag{27}$$

where

$$\begin{aligned} &C((a \leq u_g \leq b, c \leq u_b \leq d; u_n)|u_p) = \\ &\overbrace{\qquad\qquad\qquad\qquad\qquad\qquad\qquad\qquad\qquad\qquad}^{\text{(A+B+C+D)}} \\ &C_{g,b|p,n}(C_{g|p,n}(C_{g|p}(b|u_p)|C_{n|p}(u_n|u_p), C_{b|p,n}(C_{b|p}(d|u_p)|C_{n|p}(u_n|u_p))) + \\ &\overbrace{\qquad\qquad\qquad\qquad\qquad\qquad\qquad\qquad\qquad\qquad}^{\text{C}} \\ &+ C_{g,b|p,n}(C_{g|p,n}(C_{g|p}(a|u_p)|C_{n|p}(u_n|u_p), C_{b|p,n}(C_{b|p}(c|u_p)|C_{n|p}(u_n|u_p))) - \\ &\overbrace{\qquad\qquad\qquad\qquad\qquad\qquad\qquad\qquad\qquad\qquad}^{\text{(C+D)}} \\ &- C_{g,b|p,n}(C_{g|p,n}(C_{g|p}(a|u_p)|C_{n|p}(u_n|u_p), C_{b|p,n}(C_{b|p}(d|u_p)|C_{n|p}(u_n|u_p))) - \\ &\overbrace{\qquad\qquad\qquad\qquad\qquad\qquad\qquad\qquad\qquad\qquad}^{\text{(C+B)}} \\ &- C_{g,b|p,n}(C_{g|p,n}(C_{g|p}(b|u_p)|C_{n|p}(u_n|u_p), C_{b|p,n}(C_{b|p}(c|u_p)|C_{n|p}(u_n|u_p))) \end{aligned} \tag{28}$$

with $a = 0.5 - \frac{\beta}{2}$, $b = 0.5 + \frac{\beta}{2}$, $c = 0.5 - \frac{\alpha}{2}$ and $d = 0.5 + \frac{\alpha}{2}$.

In Fig. 5, x and y-axis report the conditional distribution of brown and green assets, given neutral ones and physical risk index, respectively. Graphically, our area of interest is colored in blue and denoted with the letter A. Clearly, determining this area consists in computing the difference between areas $(A+B+2C+D)$, $B+C$ and $D+C$. The C area is both summed and subtracted twice, reflecting the inherent nature of a copula as a joint cumulative distribution function, which accounts for the cumulative probabilities across multiple dimensions of the variables involved.

Regarding the financial institutions, expanding the approach of Ojea-Ferreiro et al. (2024), we assume the dependence between bank i and climate variables through the copulas $C_{gi|pn}(u_g|(u_p, u_n), i)$ and $C_{bi|pn}(u_b|(u_p, u_n), i)$. The cascading effects of climate risks on the financial system are analyzed at an institutional level, one bank at a time for each climate state $\mathcal{C}$. Consequently, risk metrics (C-ER, C-VAR and C-ES) are estimated separately for each institution in the first place. The procedure has been implemented in MATLAB estimating the copula function with maximum likelihood procedures and solving the integrals of equations 9, 12 and 13 numerically. We employed MATLAB 2025a running on a Windows system equipped with an Intel(R) Core(TM) i9-14900K processor (3.20 GHz) and 32 GB of RAM.

In order to get an aggregate measure of climate risk at both country and European levels, risk metrics are combined afterwards, either by additive aggregation or by looking at central tendencies to capture the overall behavior of the financial sector.

6 Empirical results

In this section, we discuss the results for climate stress testing by presenting first the results of the marginal distribution from which we obtain the inputs for the copula and from which we assess the quantile for the conditioning variables. Later, we discuss the results for the copula estimations and copula choice, from which we assess the conditional quantile. Finally, we discuss climate risk metrics, *i.e.* C-ER, C-VAR, C-ES and CRISK, both at bank and systemic level (country or European).

6.1 Marginal distributions

In this study, in order to compute the joint density function of banks and climate variables, we employ the method of Inference Functions for Margins ("IFM"), that is a two step procedure introduced by Joe and Xu (1996). More specifically, to estimate parameters through the maximization of the log-likelihood function, marginal distributions and copulas are estimated separately. The starting point of our analysis is the estimation of the marginal models of bank returns' distributions and climate indexes. For each financial institution and for green, neutral and brown indexes, we estimate ARMA(p,q) processes up to (5,5)-order, where p and q represent the number of auto-regressive (AR) and moving average (MA) lags, respectively. Moreover, we estimate heteroskedasticity and leverage effect by testing some GJR-GARCH processes up to (2,2,2)-order. Optimal orders of ARMA and GJR-GARCH models have been selected by choosing those presenting the lowest BIC. Finally, skewness and kurtosis of returns have been modeled by assuming a Hansen's *skew-t* distribution. More specifically, for each financial institution i and for green, neutral and brown indexes, we estimate ARMA(p,q) processes, *i.e.*:

$$r_{i,t} = \phi_{i,0} + \sum_{j=1}^{p} \phi_{i,j} r_{i,t-j} + \sum_{k=1}^{q} \psi_{i,k} \epsilon_{i,t-k} + \epsilon_{i,t} \tag{29}$$

up to (5,5)-order, where:

1. $\sum_{i=1}^{p} \phi_i y_{t-i}$ represents the auto-regressive component (AR), and p is the maximum number of auto-regressive lags;
2. $\sum_{j=1}^{q} \theta_j \epsilon_{t-j}$ represents the moving average component (MA), and q is the maximum number of moving average lags;
3. $\epsilon_{n,t}$ is given by $\sigma_{n,t}\xi_{n,t}$. Moreover, $E(\epsilon_{n,t}, \epsilon_{n,t-k}) = 0$ with $k \neq 0$, *i.e.* residuals, on average, are not auto-correlated.

Moreover, we estimate heteroskedasticity and leverage effect by testing different GJR-GARCH(p,o,q) processes up to (2,2,2)-order, *i.e.*:

$$\sigma_{i,t}^2 = \omega_i + \sum_{j=1}^{p} \alpha_{i,j} \epsilon_{i,t-j}^2 + \sum_{k=1}^{o} \gamma_{i,k} \epsilon_{i,t-k}^2 I_{\{\epsilon_{i,t-k}<0\}} + \sum_{m=1}^{q} \beta_{i,m} \sigma_{i,t-m}^2 \tag{30}$$

where:

1. $\sigma_{i,t}^2$ is the conditional variance for return i at time t,
2. ω_i is the constant term,
3. $\alpha_{i,j}$ are the coefficients for the ARCH term (*i.e.* $\sum_{j=1}^{p} \alpha_{i,j} \epsilon_{i,t-j}^2$), which represent the effect of past squared residuals on the current conditional variance $\sigma_{i,t}^2$,

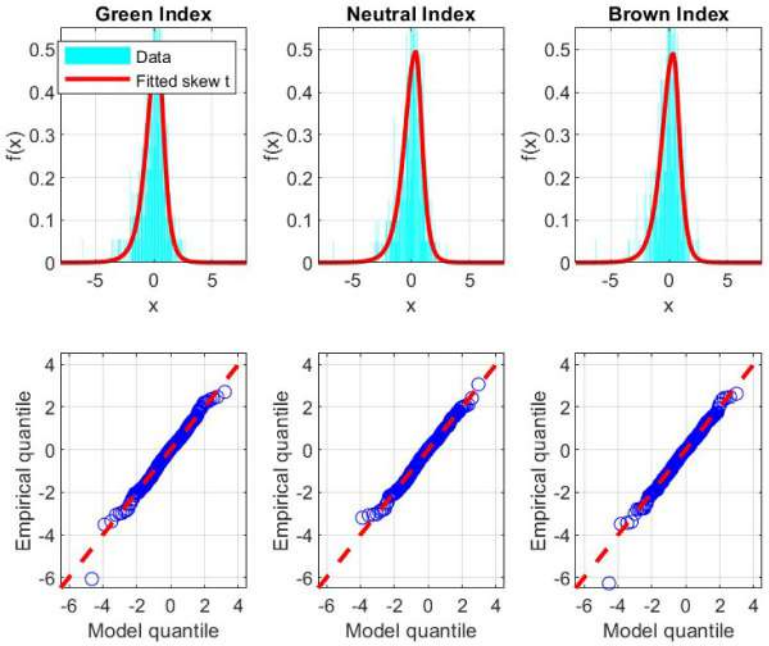

The upper panels of this figure present the fitted Hansen's skew t density for the green, neutral and brown indexes standardized residuals, along with histograms of these residuals; the lower panels present QQ plots.

Fig. 6 Empirical and fitted distributions for green, neutral and brown indexes

4. $\gamma_{i,k}$ are the coefficients for the leverage effect (*i.e.* $\sum_{k=1}^{o} \gamma_{i,k} \epsilon_{i,t-k}^2 I_{\{\epsilon_{i,t-k}<0\}}$), which capture the tendency for volatility to rise more following a large price fall than following a price rise of the same magnitude,
5. $I_{\{\epsilon_{i,t-k}<0\}}$ is an indicator function that equals 1 if $\epsilon_{i,t-k} < 0$ and 0 otherwise,
6. $\beta_{i,m}$ are the coefficients for the GARCH term (*i.e.* $\sum_{m=1}^{q} \beta_{i,m} \sigma_{i,t-m}^2$), which represent the effect of past conditional variances on the current conditional variance $\sigma_{i,t}^2$.

In particular, we tested six different GJR-GARCH models, allowing also for asymmetry. Univariate volatility models tested are (1,0,0), (1,0,1), (1,1,1), (2,0,0), (2,0,2) and (2,2,2).

In modeling residuals, we assume $\xi_{n,t} \sim \text{ST}(\xi_{n,t}; \nu_n, \lambda_n)$ where ST indicates the Hansen's *skew-t* distribution, with ν degrees of freedom ($2 < \nu < \infty$) and asymmetry parameter λ ($-1 < \lambda < 1$). The following figure reports for green, neutral and brown indexes the empirical and fitted distributions (Fig. 6).

6.2 Copula functions

As far as the market is concerned, *i.e.* the relation between physical risk vs green, neutral and brown companies in the first tree and between green and brown vs neutral companies (conditioned on physical risk) in the second tree, for each pair of variables we considered 8 different types of copulas, commonly employed in financial studies. Each copula differs

in tail dependence characteristics[13]. For example, the Clayton and the Survival Gumbel copulas allow for lower tail dependence but no upper tail dependence, whereas the opposite situation is found in Gumbel and Survival Clayton copulas. Finally, other copulas, such as the symmetrised Joe-Clayton (BB7)[14] and the Student's t copulas, allow for either upper and lower tail dependence.

In this work, we assume that the functional form of the copula remains fixed over time, allowing the set of parameters $\boldsymbol{\Theta}$ varying dynamically based on some equations for time evolution. In literature, there exist several alternative approaches to model time-varying copula parameters. For example, Aloui et al. (2013) rely on the use of rolling-windows, while others, such as Creal et al. (2013) and Hafner and Manner (2012), on the use of a Generalized Autoregressive Score ("GAS") or Stochastic Autoregressive Copulas ("SCAR"). In the present study, equations that characterize the time dependency have been retrieved from Patton (2006b)[15].

For each copula we have computed the negative sum of log-likelihood (NSLL), the Akaike Information Criterion (AIC) and the Bayesian Information Criterion (BIC) and selected that showing the most negative BIC. Copula estimation reveals that green, neutral, and brown companies exhibit the best fit with physical risk *via* a Gaussian copula structure. Furthermore, conditional on the physical risk index, both green and brown firms show asymmetric tail dependence with neutral firms, which is best captured by a rotated Gumbel copula.

When financial institutions are taken into consideration, *i.e.* when we analyze the dependency of green and brown companies (conditional on neutral ones and physical risk) vs European banks, the number of tested copulas has been restricted to four (Gaussian, Student's t, Gumbel and Clayton copulas). The analysis points out that most financial firms exhibit statistical independence from green firms (conditional on neutral ones and physical risk index), while showing significant dependence on brown firms (conditional on neutral ones and physical risk index), best characterized by a Gaussian copula. In marginal cases, the dependence structure is better captured by a Gumbel copula, suggesting asymmetric upper tail dependence.

6.3 C-ER, C-VAR, C-ES results

In this section, we present the estimations of C-ER, C-VAR and C-ES of the sample in analysis under the three assumed climate scenarios. Results are examined both on a granular and on a systemic level. In order to come to systemic measure of climate risk, results are summarized with measures of central tendency.

Figure 7a depicts C-ER average results under the assumption of a disorderly transition scenario (solid green line), orderly transition scenario (blue dotted line) and a hot house world scenario (red dotted line). More specifically, for each scenario, Fig. 7a depicts the dynamic of the weekly average C-ER from 2014 to 2023. At each time t, average values have been obtained by weighting individual C-ER$_i$ results for the respective market capitalization.

[13] Given two random variables X_1 and X_2, we define $F_{X_1}^{-1}$ and $F_{X_2}^{-1}$ their quantile functions. The lower tail dependence coefficient λ_L is defined by $\lambda_L := \lim_{t\to 0^+} Pr(X_2 \leq F_{X_2}^{-1}(t) | X_1 \leq F_{X_1}^{-1}(t))$, provided that the limit $\lambda_L \in [0, 1]$ exists. Analogously, λ_U is defined as $\lambda_U := \lim_{t\to 1^-} Pr(X_2 > F_{X_2}^{-1}(t) | X_1 > F_{X_1}^{-1}(t))$, provided that the limit $\lambda_L \in [0, 1]$ exists. If $0 < \lambda_L \leq 1$ ($0 < \lambda_U \leq 1$), then X_1 and X_2 are said to be *asymptotically dependent* in the lower (upper) tail.

[14] See Patton (2006b).

[15] For more details on the employed equations, see Appendix A.

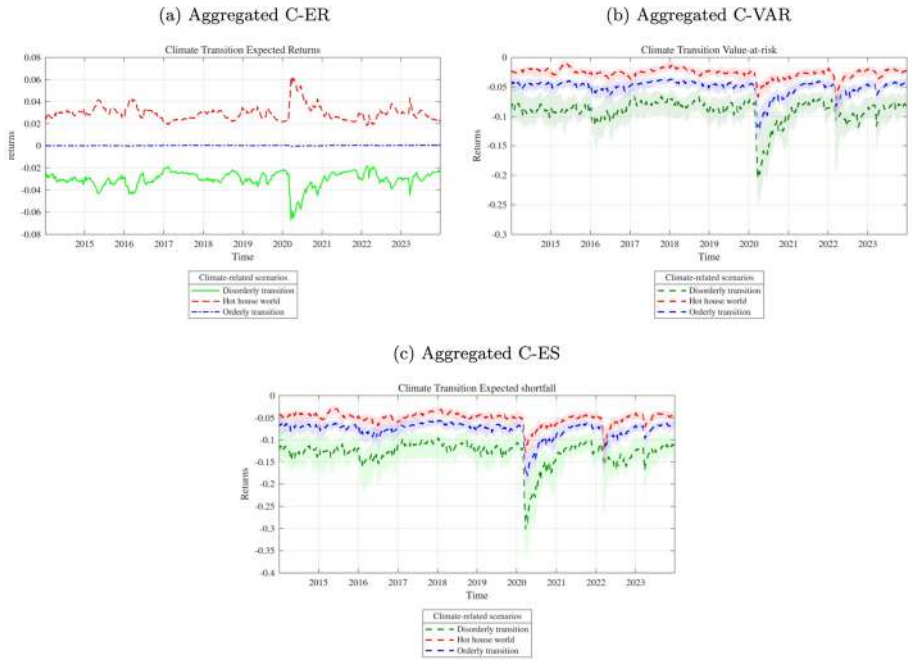

Fig. 7 Aggregated C-ER, C-VAR and C-ES results. Figure 7a, 7b and 7c report C-ER, C-VAR and C-ES of the European financial system under the disorderly transition, the orderly transition and the hot house world. The disorderly transition is represented by the green line, while the hot house world and the orderly transition from the red and blue ones, respectively. At each time t, C-ER average values have been obtained by weighting individual C-ER results for the respective market capitalization. Concerning C-VAR and C-ES, for each time t, we report the median value along with the 25th and the 75th percentiles of the respective distributions

At a European level, the financial system presents a strong dependency from brown companies, and this is confirmed by the strong positive return, consistently higher than 2%, that the system would register in case of materialization of the how house world scenario.

Figures 7b and 7c depict, for each time t from 2014 to 2023, the median C-VAR and C-ES, respectively. The choice of the median value instead of the weighted average reflects the different nature of C-VAR and C-ES with respect to C-ER. As a matter of fact, differently from C-ER, which can be treated as an additive measure, C-VAR and C-ES cannot. In order to give a summary representation of C-VAR and C-ES distributions, along with median values, the 25^{th} and the 75^{th} percentiles of the respective distributions are reported. In each picture, the two percentiles correspond to the upper and lower borders of the shaded area. Interestingly, C-VAR generally points out greater losses in the hot house world scenario than in the orderly transition and in the disorderly transition scenario. Results are not confirmed in terms of C-ES, from which it emerges greater losses in the disorderly scenario. While C-VAR and C-ES values remain quite stable during the period in analysis, an abrupt drop appears during Covid pandemic and the energetic crisis, reflecting a risk increase in all the scenarios.

Table 4 reports the estimations of C-ER, C-VAR and C-ES of each bank for the disorderly transition, the orderly transition and the hot house world scenario.

Clearly, the individual outcomes depend on a variety of factors, including company-specific performances, strategic investment allocations, loan portfolio composition, and the

Table 4 Granular C-ER, C-VAR and C-ES results

Banks	Disorderly transition			Orderly transition			Hot house world		
	C-ER	C-VAR	C-ES	C-ER	C-VAR	C-ES	C-ER	C-VAR	C-ES
Credit Agricole SA	−0.0280	−0.0890	−0.1391	0.0013	−0.0454	−0.0753	0.0262	−0.0183	−0.0407
BNP Paribas SA	−0.0353	−0.0984	−0.1488	0.0008	−0.0445	−0.0727	0.0297	−0.0128	−0.0350
Societe Generale SA	−0.0392	−0.1103	−0.1647	−0.0002	−0.0527	−0.0848	0.0320	−0.0184	−0.0430
Banco Santander SA	−0.0418	−0.1035	−0.1487	−0.0007	−0.0475	−0.0718	0.0381	−0.0134	−0.0337
Banco Bilbao Vizcaya Argentaria SA	−0.0377	−0.0934	−0.1300	0.0001	−0.0446	−0.0666	0.0360	−0.0127	−0.0312
ING Groep NV	−0.0468	−0.1142	−0.1509	0.0011	−0.0424	−0.0614	0.0491	−0.0155	−0.0450
UniCredit SpA	−0.0540	−0.1217	−0.1580	0.0008	−0.0589	−0.0854	0.0527	−0.0074	−0.0305
Intesa Sanpaolo SpA	−0.0299	−0.0841	−0.1172	0.0011	−0.0449	−0.0679	0.0299	−0.0175	−0.0370
Commerzbank AG	−0.0412	−0.1099	−0.1475	0.0004	−0.0622	−0.0890	0.0434	−0.0268	−0.0511
Deutsche Bank AG	−0.0393	−0.1055	−0.1387	−0.0011	−0.0603	−0.0859	0.0362	−0.0270	−0.0510
DNB Bank ASA	−0.0223	−0.0704	−0.0928	0.0011	−0.0429	−0.0623	0.0226	−0.0217	−0.0402
Danske Bank A/S	−0.0089	−0.0534	−0.0804	−0.0002	−0.0407	−0.0639	0.0339	−0.0251	−0.0473
Erste Group Bank AG	−0.0255	−0.0778	−0.1128	0.0012	−0.0441	−0.0680	0.0269	−0.0208	−0.0407
KBC Group NV	−0.0233	−0.0730	−0.1009	0.0010	−0.0431	−0.0647	0.0236	−0.0197	−0.0387
Swedbank AB	−0.0105	−0.0577	−0.0924	0.0004	−0.0406	−0.0674	0.0105	−0.0300	−0.0531
Raiffeisen Bank International AG	−0.0376	−0.1057	−0.1523	0.0002	−0.0557	−0.0845	0.0373	−0.0249	−0.0482
Banco BPM SpA	−0.0422	−0.1229	−0.1678	0.0003	−0.0720	−0.1059	0.0410	−0.0328	−0.0629
Mediobanca Banca di Credito Finanziario SpA	−0.0207	−0.0790	−0.1114	0.0018	−0.0486	−0.0750	0.0217	−0.0246	−0.0479
BPER Banca SPA	−0.0362	−0.1101	−0.1471	0.0003	−0.0666	−0.0967	0.0353	−0.0317	−0.0592
Jyske Bank A/S	−0.0075	−0.0684	−0.1128	0.0007	−0.0380	−0.0582	0.0404	−0.0456	−0.0900
Powszechna Kasa Oszczednosci Bank Polski SA	−0.0243	−0.0766	−0.1083	0.0007	−0.0475	−0.0711	0.0251	−0.0252	−0.0462

Table 4 continued

Banks	Disorderly transition			Orderly transition			Hot house world		
	C-ER	C-VAR	C-ES	C-ER	C-VAR	C-ES	C-ER	C-VAR	C-ES
Bank Polska Kasa Opieki SA	−0.0203	−0.0715	−0.1009	0.0002	−0.0478	−0.0712	0.0202	−0.0291	−0.0502
Banca Popolare di Sondrio SPA	−0.0265	−0.0863	−0.1316	0.0016	−0.0496	−0.0788	0.0290	−0.0264	−0.0500
Bank of Ireland Group PLC	−0.0275	−0.0904	−0.1183	0.0010	−0.0602	−0.0850	0.0293	−0.0342	−0.0582
Banco Comercial Portugues SA	−0.0487	−0.1335	−0.1889	−0.0021	−0.0727	−0.1078	0.0436	−0.0316	−0.0611
Skandinaviska Enskilda Banken AB	−0.0124	−0.0601	−0.0881	0.0010	−0.0417	−0.0654	0.0133	−0.0270	−0.0478
Sydbank AS	−0.0145	−0.0617	−0.0960	0.0018	−0.0416	−0.0669	0.0176	−0.0261	−0.0467
Banca Monte dei Paschi di Siena SpA	−0.0415	−0.1266	−0.2293	−0.0111	−0.0838	−0.1453	0.0180	−0.0601	−0.1064
CaixaBank SA	−0.0370	−0.0946	−0.1259	0.0001	−0.0510	−0.0738	0.0366	−0.0169	−0.0372
AIB Group PLC	−0.0340	−0.1060	−0.1646	−0.0015	−0.0648	−0.1026	0.0307	−0.0354	−0.0640
Ringkjoebing Landbobank A/S	0.0062	−0.0230	−0.0378	0.0041	−0.0255	−0.0411	−0.0113	−0.0545	−0.0916
Santander Bank Polska SA	−0.0161	−0.0680	−0.0948	0.0011	−0.0499	−0.0727	0.0184	−0.0328	−0.0532
HSBC Holdings PLC	−0.0224	−0.0628	−0.0899	−0.0002	−0.0351	−0.0527	0.0217	−0.0161	−0.0306
Barclays PLC	−0.0339	−0.1115	−0.1692	−0.0006	−0.0472	−0.0711	0.0298	−0.0377	−0.0791
NatWest Group PLC	−0.0366	−0.1136	−0.1763	−0.0004	−0.0485	−0.0739	0.0340	−0.0382	−0.0838
Bankinter SA	−0.0267	−0.0812	−0.1110	0.0011	−0.0445	−0.0665	0.0275	−0.0185	−0.0379
Standard Chartered PLC	−0.0334	−0.0923	−0.1371	−0.0009	−0.0485	−0.0753	0.0295	−0.0200	−0.0409
Banco de Sabadell SA	−0.0472	−0.1213	−0.1734	−0.0001	−0.0618	−0.0928	0.0464	−0.0224	−0.0478
Lloyds Banking Group PLC	−0.0271	−0.0864	−0.1266	−0.0007	−0.0395	−0.0576	0.0275	−0.0339	−0.0656
Nordea Bank Abp	−0.0156	−0.0608	−0.0896	0.0006	−0.0400	−0.0622	0.0160	−0.0238	−0.0426
Svenska Handelsbanken AB	−0.0144	−0.0569	−0.0806	0.0000	−0.0399	−0.0591	0.0142	−0.0269	−0.0438
Banque Cantonale Vaudoise	0.0084	−0.0180	−0.0315	0.0022	−0.0244	−0.0395	−0.0044	−0.0325	−0.0508
UBS Group AG	−0.0185	−0.0635	−0.0938	0.0016	−0.0386	−0.0603	0.0211	−0.0218	−0.0399

This table reports the C-ER, C-VAR and C-ES of individual banks under each climate scenario (namely the disorderly transition, the orderly transition and the hot house world)

type of copula model identified as the best fitting the underlying data. In addition, these outcomes are not static, since they reflect not only structural and financial features of various institutions but also the banks' responsiveness and adaptability to the unfolding realities of the eventual climate outcome. The speed and efficiency with which banks conform to these scenarios play, of course, a crucial role in determining their risk exposure, therefore underlining the interplay between preparedness, strategic agility, and systemic challenges posed by climate transition.

Consistently with the strong dependence of financial institutions to brown companies, the European financial system would benefit greatly in a hot world scenario, in which almost all the financial institutions in the sample would register positive C-ER, up to +0.05 (Unicredit). In contrast, the disorderly transition scenario would worsen general performances, with strong negative results up to -0.05 (Unicredit). In the orderly transition scenario, returns are stably low and approximately equal to 0%. This trend is not always confirmed from the analysis of C-ER on a bank specific basis. In some cases (*i.e.* Ringkjoebing Landbobank A/S and Banque Cantonale Vaudoise), the opposite dynamic holds, with an average positive return in case of a disorderly transition scenario and an average negative return in case of a hot house world scenario.

Interesting insights about climate systemic risk come from the analysis of the aforementioned financial metrics on a country-level aggregation. In Appendix E, F, and G, the dynamic of country C-ER, C-ES and C-VAR is reported, from which it emerges that the systemic impact on European banks of a disorderly transition scenario is much more severe than the impact of the orderly transition scenario and the hot house world; this is particularly evident during the Covid pandemic period and the following Russian war.

Table 5 depicts the systemic impact of the three climate transition scenarios on the European countries included in our sample. Here we report results just for France, Spain, Italy, Germany, Norway and UK. For each climate scenario, we assess the central tendency of country-level financial firms' climate risk exposure by aggregating the results for C-ER, C-VAR, and C-ES. The empirical results confirm that, in nearly all countries considered, the financial system exhibits a high level of risk exposure under a low-carbon transition scenario. Overall, under a disorderly transition scenario C-ES registers negative returns up to -15%. Conversely, in case of a hot house world scenario, the financial system of most relevant European countries would benefit, given that banks show a high exposure towards brown companies. Taking France as a reference, the estimated values of C-ER, C-VAR, and C-ES under the disorderly transition scenario are -0.0350, -0.1025, and -0.1559, respectively, compared with 0.0298, -0.0199, and -0.0447 under the hot house world scenario. Given the actual policy framework, which penalizes brown companies by transitioning towards a low-carbon economy, the evidence suggests the need for adjustments in portfolio management strategies, specifically by mitigating exposures to brown companies and increasing allocations towards green companies. Results are reported graphically in Appendixes E, F and G.

6.4 CRISK results

In this section, we try to assess the implication of each climate scenario (disorderly transition, orderly transition and hot house world) in terms of capital at risk for each European country.

It is reasonable to assume that each climate scenario determines a different impact on bank performances and, hence, stock returns, depending on their exposure to specific sectors. This type of risk is generally denominated market risk, which is measured in terms of value changes of financial instruments held by a bank due to unexpected changes in market conditions. For

Table 5 Country-level C-ER, C-VAR and C-ES results

Banks	Disorderly transition			Orderly transition			Hot house world		
	C-ER	C-VAR	C-ES	C-ER	C-VAR	C-ES	C-ER	C-VAR	C-ES
France	−0.0350	−0.1025	−0.1559	0.0007	−0.0494	−0.0819	0.0298	−0.0199	−0.0447
Spain	−0.0408	−0.1029	−0.1436	−0.0003	−0.0524	−0.0771	0.0385	−0.0198	−0.0414
Italy	−0.0403	−0.1145	−0.1530	0.0006	−0.0653	−0.0948	0.0392	−0.0289	−0.0543
Germany	−0.0414	−0.1126	−0.1496	−0.0007	−0.0653	−0.0934	0.0398	−0.0292	−0.0549
Norway	−0.0229	−0.0752	−0.0997	0.0010	−0.0469	−0.0681	0.0231	−0.0238	−0.0439
UK	−0.0283	−0.1007	−0.1493	−0.0005	−0.0520	−0.0785	0.0267	−0.0409	−0.0790

This table reports the C-ER, C-VAR and C-ES for each country under each climate scenario. The country C-ER is the mean of individual C-ER weighted for market capitalization. Country C-VAR and country C-ES are computed as the median of individual average metrics.

instance, banks with a relevant exposure to green companies are supposed to benefit of an increase in asset value under a disorderly transition scenario, in which green firms have a relative advantage with respect brown companies. On the other hand, when a hot house world is assumed, brown companies are going to experience a relative advantage with respect green firms and this in turn could have an impact on value of banks heavily exposed to brown sectors.

Figures 8a, 8b and 8c reports CRISK of European countries in each of the three climate scenarios. Sizable differences in climate risk emerge, depending on the climate scenario assumed. In particular, CRISK reaches its minimum in the hot house world scenario and its maximum under the orderly transition scenario, as banks tend to benefit from their relatively higher exposures to brown companies, which perform better without a low-carbon transition, as highlighted in previous sections. European CRISK would reach approximately EUR 120 bn by the end of 2023 under a disorderly transition scenario. The greatest contribution to climate systemic risk comes from France (EUR 30 bn), followed by UK (EUR 28 bn). Limited impacts are registered by Spain, Italy and Germany (EUR 16 bn, EUR 10 bn and EUR 9 bn respectively). These results can be compared with those obtained in a previous contribution (Giacchetta et al., 2024). In that paper, we quantify the European CRISK in a disorderly transition setting through the use of dynamic conditional correlation model. More specifically, we register an increasing climate CRISK and a still sizable climate risk by the end of 2023 (the aggregated European CRISK is quantified in about EUR 160 bn). We conclude by examining countries contribution, with most of it coming from France for about EUR 100 bn, followed by UK (EUR 37 bn). In contrast, different CRISK dynamic is shown by Norwegian banks, which seem to be unaffected by climate risk. On the other hand, a moderate exposure to climate risk appears in case of orderly transition scenario, quantifiable in approximately EUR 50 bn at the end of 2023. Again, France would be the greatest contributor (EUR 21 bn), together with UK (EUR 16 bn), Germany (EUR 6 bn) and Spain (EUR 5 bn). This is not the case of the hot house world scenario, under which the European banking system would appear almost entirely immune to climate risk. All in all, the empirical results show a persistent yet manageable capital shortfall related to climate risk, even in the most adverse scenario (namely the disorderly transition). Considering the market capitalization of our sample at the end of 2023, equal to EUR 1.100 bn, CRISK can be quantified in about 11% of the capital in the disorderly transition scenario, 5% in the orderly transition scenario and negligible in the hot house world scenario.

7 Conclusions

In this paper, we quantify the climate risk exposure of a large sample of European banks under three NGFS-aligned climate scenarios. In particular, we expand the methodology of Ojea-Ferreiro et al. (2024), which involve the use of vine copulas to construct climate scenario. Differently from Ojea-Ferreiro et al. (2024), in this study the climate transition risk perspective has been integrated with the physical one. This allows us to characterize scenarios in terms of different combination of climate risks.

In particular, climate risk exposure is measured assuming three distinct climate scenarios: disorderly transition, orderly transition and hot house world. In each of these scenarios, the exposure to climate risk of the financial system is assessed through the computation of four relevant risk metrics: the conditional expected return C-ER, the conditional value-at-risk C-VAR, the conditional expected shortfall C-ES and, finally, the CRISK.

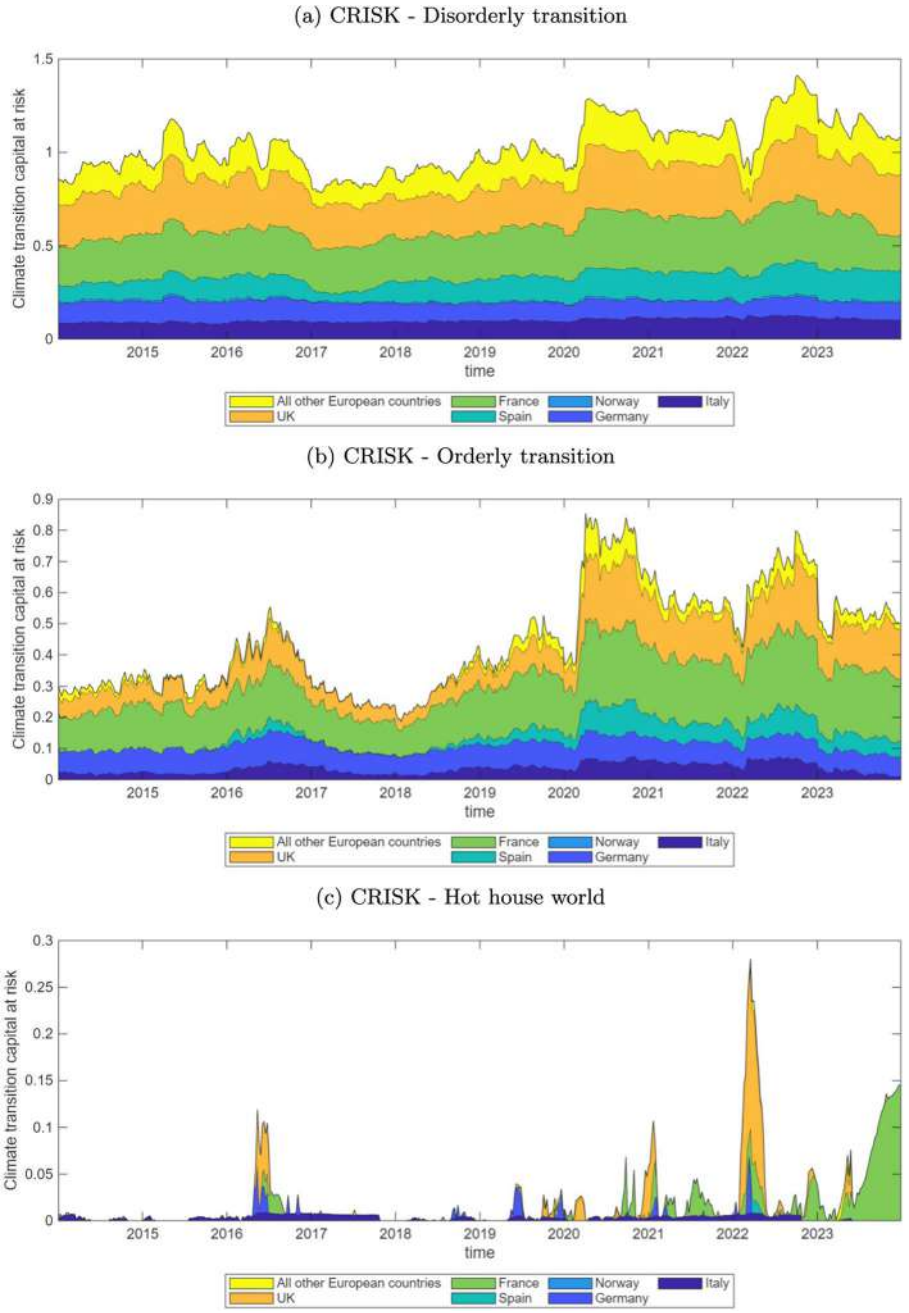

Fig. 8 Aggregated CRISK of the European financial system in different scenarios. These figures depict the dynamic of country CRISK assuming different climate scenarios between 2014 and 2023. The capital shortfall results particularly pronounced under the disorderly climate transition scenario, reflecting the higher financial vulnerabilities that arise in the light of abrupt and uncoordinated policy changes toward low-carbon economies

In general, results vary from country to country. However, they confirm a high exposure of European banks towards brown sectors. We have evidence of an increasing CRISK during years 2022-2023, with a sizable relevance in the disorderly transition scenario (EUR 120 bn at European level by the end of 2023). The results are particularly relevant for authorities and central regulators, since market authorities need a quantitative analysis of the impact of climate change on the financial system. The existence of capital shortfalls, when a specific climate scenario occurs, motivates policy actions taken by the regulator. Moreover, CRISK offers valuable insights into the current state of the European financial system by identifying the banks most vulnerable to adverse climate scenarios and, when necessary, indicating the need for additional capital injections.

Appendix A: Parameter equations for time dependency

In the present study, following Patton (2006b), for Gaussian and Student's t copulas, the dynamic of the parameter ρ has been assumed equal to:

$$\rho_t = \Lambda_1 \left(\omega + \beta \rho_{t-1} + \alpha \frac{1}{10} \sum_{k=1}^{10} \phi^{-1}(u_{1,t-k}) \cdot \phi^{-1}(u_{2,t-k}) \right) \tag{A1}$$

where ϕ^{-1} denotes the inverse Gaussian cumulative distribution in case of Gaussian copulas and the inverse Student's t cumulative distribution in case of Student's t copulas. In this context, we assume $\Lambda_1(x) = \frac{1.998}{1+\exp(-x)} - 0.999$, *i.e.* a logistic transformation functional to keep the dependence coefficient between -1 and 1. For Student's t copulas, degrees of freedom have been allowed to change dynamically following the equation:

$$\eta_t = \Lambda_2 \left(\omega + \beta \eta_{t-1} + \alpha \frac{1}{10} \sum_{k=1}^{10} \phi^{-1}(u_{1,t-k}) \cdot \phi^{-1}(u_{2,t-k}) \right) \tag{A2}$$

where $\Lambda_2(x) = \frac{\exp(x)}{1+\exp(x)} \cdot 98 + 2$.

Finally, for the Gumbel and Clayton copulas, we adopted the following parametric representation:

$$\theta_t = \Lambda_2 \left(\omega + \beta \theta_{t-1} + \alpha \frac{1}{10} \sum_{k=1}^{10} \phi^{-1}(u_{1,t-k}) \cdot \phi^{-1}(u_{2,t-k}) \right) \tag{A3}$$

Appendix B: OLS regression of bank stocks' returns vs green, neutral and brown indexes

See Table 6

Table 6 The figure reports the OLS regression result of banks' stock against green, brown and neutral index, as well as the EURO STOXX 600 index as controlling variable. T-stats reported in the table have been computed by bootstrapping residuals 10.000 times. From the analysis conducted, it emerges that European financial institutions are heavily exposed to brown companies, with an average β_{brown} equal to 1.53. On the other hand, exposure to green and neutral appears to be low and not always statistically significant

Banks	Int.	T-stat	Green	T-stat	Neutral	T-stat	Brown	T-stat	SPXX	T-stat
aca	0.0011	0.7923	−0.1566	−0.6900	−0.7815	−2.0012	0.9747	4.5304	1.2910	3.9392
bnp	0.0004	0.3229	0.4271	1.9377	−1.6126	−4.2650	1.4076	6.8634	1.0483	3.3556
gle	−0.0006	−0.3625	0.4772	1.8038	−1.6762	−3.6614	1.7994	7.2232	0.8249	2.1826
san	0.0002	0.1217	0.1813	0.7523	−2.2824	−5.5166	1.5935	7.1265	1.7658	5.2428
bbva	0.0008	0.5588	−0.0437	−0.1913	−1.6131	−4.0850	1.5791	7.3348	1.3093	4.0336
inga	0.0009	0.6940	0.1852	0.8559	−1.2822	−3.4506	1.4979	7.2906	0.9749	3.1176
ucg	0.0019	0.9825	−0.6210	−1.9760	−1.5837	−2.9156	0.8147	2.7457	2.7583	6.0074
isp	0.0013	0.9103	0.1153	0.4894	−1.5288	−3.7553	0.6885	3.1562	1.9427	5.8114
cbk	0.0013	0.6534	0.1723	0.5222	−1.9211	−3.4038	2.0215	6.6027	1.0766	2.2869
dbk	−0.0007	−0.4119	0.5636	1.9502	−2.4843	−5.0001	1.3712	4.9651	1.9453	4.6730
dnb	0.0006	0.4800	0.4459	2.2370	−1.0631	−3.1137	1.3121	6.9680	0.4032	1.3974
danske	0.0005	0.3366	0.2920	1.3714	−0.3118	−0.8544	1.3188	6.5608	−0.4245	−1.3701
ebs	0.0007	0.4267	0.2832	1.0730	−0.4467	−0.9802	1.6145	6.4560	−0.2958	−0.7652
kbc	0.0010	0.7037	−0.0405	−0.1792	−0.6240	−1.6054	1.1938	5.6080	0.5436	1.6703
sweda	−0.0002	−0.1592	0.1153	0.5042	−0.3714	−0.9476	0.4218	1.9250	0.7660	2.2986
rbi	0.0003	0.1316	−0.4569	−1.3668	0.4262	0.7496	1.4560	4.6571	−0.1288	−0.2698
bami	0.0017	0.6865	−0.1788	−0.4368	−2.4253	−3.4542	0.9205	2.4074	2.9684	5.1357
mb	0.0010	0.6328	0.7152	2.9337	−1.5883	−3.7861	0.8684	3.8063	1.3181	3.7555

Table 6 continued

Banks	Int.	T-stat	Green	T-stat	Neutral	T-stat	Brown	T-stat	SPXX	T-stat
bpe	0.0016	0.7271	−0.5553	−1.5767	−1.5159	−2.4883	0.9962	3.0363	2.3472	4.6348
jysk	0.0011	0.7567	0.1070	0.4425	−0.4898	−1.1792	0.4963	2.1548	0.7329	2.1092
pko	0.0002	0.1356	0.0664	0.2575	0.2289	0.5139	1.0870	4.3923	−0.3771	−1.0010
peo	−0.0007	−0.4400	0.0889	0.3384	0.3978	0.8751	1.0879	4.4035	−0.4396	−1.1746
bpso	0.0018	0.9451	−0.0518	−0.1728	−0.7330	−1.4098	1.0654	3.8050	0.8418	1.9822
birg	0.0009	0.4029	1.2247	3.5171	−2.6244	−4.3285	2.0738	6.2148	0.2698	0.5352
bcp	−0.0010	−0.4246	0.0660	0.1647	−1.6850	−2.4810	2.2734	6.0815	0.5645	1.0011
seba	−0.0001	−0.0581	0.5066	2.5776	−0.5978	−1.7741	0.6901	3.7116	0.4840	1.7296
sydb	0.0015	1.0262	0.2236	0.9087	−0.7790	−1.8461	0.5746	2.5046	0.8554	2.4292
bmps	−0.0115	−3.0334	1.3718	2.2287	−3.1139	−2.9543	0.5106	0.8887	2.5155	2.8728
cabk	0.0014	0.8449	−0.1030	−0.3858	−1.7222	−3.7752	1.6785	6.7104	1.0459	2.7923
aibg	−0.0025	−0.8193	1.6459	3.3164	−1.7048	−2.0165	3.5085	7.6673	−2.5575	−3.6525
rilba	0.0021	1.9558	0.6960	4.0243	−0.6054	−2.0281	0.4563	2.8239	0.1417	0.5668
spl	0.0005	0.2710	−0.2953	−1.0211	0.7022	1.4189	1.0779	3.9783	−0.3585	−0.8693
hsba	0.0007	0.6028	−0.0375	−0.2092	−1.6799	−5.4453	0.5098	2.9989	2.0087	7.6406
barc	−0.0016	−1.0211	1.1720	4.7282	−1.9356	−4.5364	1.5181	6.4711	0.5880	1.6643
nwg	−0.0010	−0.5818	1.1263	3.9210	−2.2121	−4.4526	1.1581	4.2607	1.1799	2.8400
bkt	0.0018	1.1480	−0.3687	−1.4297	−0.5726	−1.3008	1.2674	5.2714	0.5666	1.5521
stan	−0.0000	−0.0273	0.1070	0.4151	−2.2359	−5.0182	1.3455	5.5817	1.8735	5.0867
sab	0.0012	0.5550	−0.2209	−0.6208	−1.4072	−2.3071	2.5356	7.6291	0.2859	0.5613
lloy	−0.0015	−0.9936	0.9045	3.7386	−1.2857	−3.0793	1.3452	5.9037	0.1519	0.4351
nda	−0.0001	−0.0433	0.3574	1.8577	−0.7322	−2.2290	0.6969	3.8184	0.7562	2.7525
shba	−0.0004	−0.3340	0.1557	0.7723	−0.5434	−1.5633	0.4205	2.2450	0.9283	3.2059
bcvn	0.0017	1.8221	0.4931	3.3047	−0.6646	−2.6044	−0.1959	−1.4016	0.7812	3.6985
ubsg	0.0010	0.8339	0.5731	3.0580	−1.2911	−4.0621	0.5308	3.0453	1.3933	5.2582

Appendix C: Methodological workflow

Step. 1: Construct transition risk indexes: (i) green, (ii) neutral and (iii) brown portfolios;
Step. 2: Identify a proxy for physical risk index (we rely on on the European Extreme Events Climate Index (E^3CI));
Step. 3: Determine the hierarchical structure of the implemented C-vine copula, as reported in Fig. 9, and compute climate scenarios;
Step. 4: Compute the main climate risk metrics for each bank (C-ER, C-VAR, C-ES, CRISK) under each climate scenario $\mathcal{C}$.

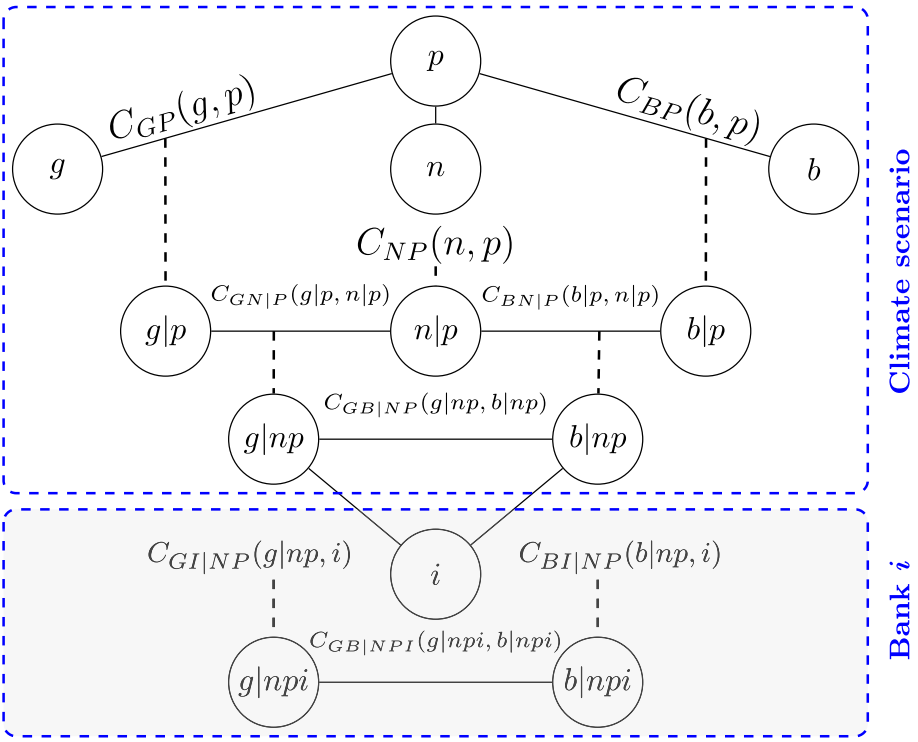

Fig. 9 Structure of the C-vine copula. The figure illustrates the structure of the C-vine copula. Nodes correspond to marginal or conditional distributions, where p denotes physical, g green, n neutral, and i bank i, while "|" indicates conditioning. Solid edges represent bi-variate copulas, whereas dotted edges denote the h-functions from which conditional distributions are derived

Appendix D: Set of bivariate copulas

Here we report the functional form of a set of bivariate copulas.

Gaussian copula. This copula depends on one parameter ρ which represents the linear correlation between the two variables. When $\rho = 1$, then the copula tail dependence is equal to 1, otherwise the copula doesn't have tail dependence. The Gaussian copula is given by the following formula:

$$C_\rho(u, v) = \Phi_2\left(\Phi^{-1}(u), \Phi^{-1}(v); \rho\right) \tag{D4}$$

where Φ_2 represents the 2-dimensional standard normal distribution function, Φ^{-1} is the inverse of the univariate standard normal distribution function an ρ is the correlation and ranges between -1 and 1. The formula D4 is not a closed formula since the Gaussian copula is an implicit copula. The Gaussian copula density function is defined as:

$$c(u, v; \rho) = \frac{1}{\sqrt{1-\rho^2}} \exp\left(-\frac{\rho^2\Phi^{-1}(u)^2 - 2\rho\Phi^{-1}(u)\Phi^{-1}(v) + \rho^2\Phi^{-1}(v)^2}{2(1-\rho^2)}\right) \tag{D5}$$

where Φ^{-1} stands for the Gaussian inverse cumulative distribution function. The conditional Gaussian copula $C_{v|u}(v|u; \rho)$ is defined as

$$H(u, v; \rho) = \frac{\partial C(u, v; \rho)}{\partial u} = \Phi\left(\frac{\Phi^{-1}(v) - \rho\Phi^{-1}(u)}{\sqrt{1-\rho^2}}\right) \tag{D6}$$

Student-t copula. The Student-t copula is defined by two parameters: ρ, which represents the correlation and η, which represents the number of degrees of freedom. This copula allows both for positive and negative tail dependence. Moreover, when $\eta \to \infty$, the Student-t copula resembles the Gaussian copula. Similarly to Gaussian copula, Student-t copula doesn't have a close form. It is represented by the following formula:

$$C_{\rho,\eta}(u, v) = T_2\left(T^{-1}(u), T^{-1}(v); \rho, \eta\right) \tag{D7}$$

where T_2 represents the 2-dimensional Student-t distribution function, T^{-1} is the inverse of the univariate Student-t distribution function, ρ is the correlation $(-1 < \rho < 1)$ and η the number of degrees of freedom. The formula D7 is not a closed formula since the Student-t copula, like the Gaussian, is defined with an implicit function.

The Student-t copula density function is defined as:

$$\begin{aligned} c(u, v; \rho, \eta) = K &\frac{1}{\sqrt{1-\rho^2}} \\ &\left[1 + \frac{T_\eta^{-1}(u)^2 - 2\rho T_\eta^{-1}(u)T_\eta^{-1}(v) + T_\eta^{-1}(v)^2}{\eta(1-\rho^2)}\right]^{-\frac{\eta+2}{2}} \\ &\left[(1+\eta^{-1}T_\eta^{-1}(u)^2)(1+\eta^{-1}T_\eta^{-1}(v)^2)\right]^{\frac{\eta+1}{2}}. \end{aligned} \tag{D8}$$

where $K = \Gamma(\frac{\eta}{2})\Gamma(\frac{\eta+1}{2})^{-2}\Gamma(\frac{\eta+2}{2})$. The conditional Student-t copula $C_{v|u}(v|u; \rho, \eta)$ is

$$H(u, v; \rho, \eta) = \frac{\partial C(u, v; \rho, \eta)}{\partial u} = T_{\eta+1}\left(\sqrt{\frac{\eta+1}{\eta + (T_\eta^{-1}(u)^2)}}\frac{T_\eta^{-1}(v) - \rho T_\eta^{-1}(u)}{\sqrt{(1-\rho^2)}}\right) \tag{D9}$$

where T_η and $T_{\eta+1}$ are the cumulative distribution function with the numbers of degrees of freedom equal to η and $eta+1$ and T_η^{-1} is the inverse of the cumulative distribution function.
Clayton copula. The Clayton copula is given by the following formula:

$$C(u, v; \theta) = \left(u^{-\theta} + v^{-\theta} - 1\right)^{-1/\theta} \tag{D10}$$

and its density function is equal to:

$$c(u, v; \theta) = (1 + \theta)\,(uv)^{-\theta-1}\left(u^{-\theta} + v^{-\theta} - 1\right)^{-2-1/\theta} \tag{D11}$$

The conditional copula with respect u is:

$$H(u, v; \theta) = \frac{\partial C(u, v; \theta)}{\partial u} = \left(u^{-\theta} + v^{-\theta} - 1\right)^{-1/\theta-1} u^{-\theta-1} \tag{D12}$$

Gumbel copula. The Gumbel copula is given by the following formula:

$$C(u, v; \theta) = \exp\left\{-\left[(-\ln u)^\theta + (-\ln v)^\theta\right]^{\frac{1}{\theta}}\right\} \tag{D13}$$

Assuming $\psi = \left[(-\ln u)^\theta + (-\ln v)^\theta\right]^{\frac{1}{\theta}}$, its density function is equal to

$$\begin{aligned} c(u, v; \theta) = {} & (\psi + \theta - 1)\psi^{1-2\theta}\exp(-\psi)\cdot \\ & \cdot (uv)^{(-1)}(-\ln u)^{(\theta-1)}(-\ln v)^{(\theta-1)} \end{aligned} \tag{D14}$$

The conditional copula with respect u is::

$$\begin{aligned} H(u, v; \theta) = \frac{\partial C(u, v; \theta)}{\partial u} = {} & \exp\left(-\left\{(-\ln u)^\theta + (-\ln v)^\theta\right\}^{\frac{1}{\theta}}\right) \\ & \left\{(-\ln u)^\theta + (-\ln v)^\theta\right\}^{\frac{1}{\theta}-1}(-\ln u)^{\theta-1}\frac{1}{u} \end{aligned} \tag{D15}$$

Plackett copula. The Plackett copula is given by the following formula:

$$C(u, v; \theta) = \frac{1 + (\theta - 1)(u + v) - \sqrt{[1 + (\theta - 1)(u + v)]^2 - 4\theta(\theta - 1)uv}}{2(\theta - 1)} \tag{D16}$$

for $\theta > 0$. When $\theta = 1$, then the Plackett copula corresponds to independence.
Its density function is equal to

$$c(u, v; \theta) == \frac{\theta\,[1 + (\theta - 1)(u + v - 2uv)]}{\left([1 + (\theta - 1)(u + v)]^2 - 4\theta(\theta - 1)uv\right)^{3/2}} \tag{D17}$$

The conditional copula with respect u is:

$$H(u, v; \theta) = \frac{\partial C(u, v; \theta)}{\partial u} = 0.5 - 0.5 \cdot \frac{1 + (-\theta - 1)v + (\theta - 1)u}{\sqrt{(1 + (\theta - 1)(v + u))^2 - 4\theta(\theta - 1)vu}} \tag{D18}$$

Frank copula. The Frank copula is given by the following formula:

$$C(u, v; \theta) = -\theta^{-1} \ln \left\{ 1 + \frac{(e^{-\theta u} - 1)(e^{-\theta v} - 1)}{e^{-\theta} - 1} \right\} \tag{D19}$$

with $-\infty < \theta < \infty$. When $\theta = 0$, then the Frank copula corresponds to independence. Its density function is equal to

$$c(u, v; \theta) = \frac{\theta e^{\theta(u+v)} \left(e^{\theta} - 1\right)}{\left[\left(e^{\theta u} - 1\right)\left(e^{\theta v} - 1\right) + e^{\theta} - 1\right]^2}, \quad \theta \neq 0. \tag{D20}$$

The conditional copula with respect u is:

$$H(u, v; \theta) = \frac{\partial C(u, v; \theta)}{\partial u} = \frac{e(-\theta u) \cdot \left(e(-\theta v) - 1\right)}{e(-\theta) - 1 + \left(e(-\theta v) - 1\right) \cdot \left(e(-\theta u) - 1\right)} \tag{D21}$$

Symmetrised Joe-Clayton copula. The Symmetrised Joe-Clayton copula is a slight modification of the original Joe-Clayton copula (also known as BB7 copula) proposed by Patton (2006b). It is given by the following formula:

$$C(u, v; \tau^U, \tau^L) = 1 - \left(1 - \left\{[1 - (1 - u)^k]^{\gamma} + [1 - (1 - v)^k]^{-\gamma} - 1\right\}^{-\frac{1}{\gamma}}\right)^{-\frac{1}{k}} \tag{D22}$$

where $k = \frac{1}{\log_2(2-\tau^U)}$, $\gamma = -\frac{1}{\log_2(\tau^L)}$ and $0 < \tau^U < 1, 0 < \tau^L < 1$.
Its density function is equal to:

$$C_{SJC}(u, v; \tau^U, \tau^L) = 0.5 \cdot (C_{JC}(u, v; \tau^U, \tau^L) + C_{JC}(1 - u, 1 - v; \tau^L, \tau^U) + u + v - 1) \tag{D23}$$

More information about Joe-Clayton copula can be found in Patton (2006b), Patton (2004) and Patton (2006a).

Appendix E: Country C-ER for disorderly transition, orderly transition and hot house world scenarios

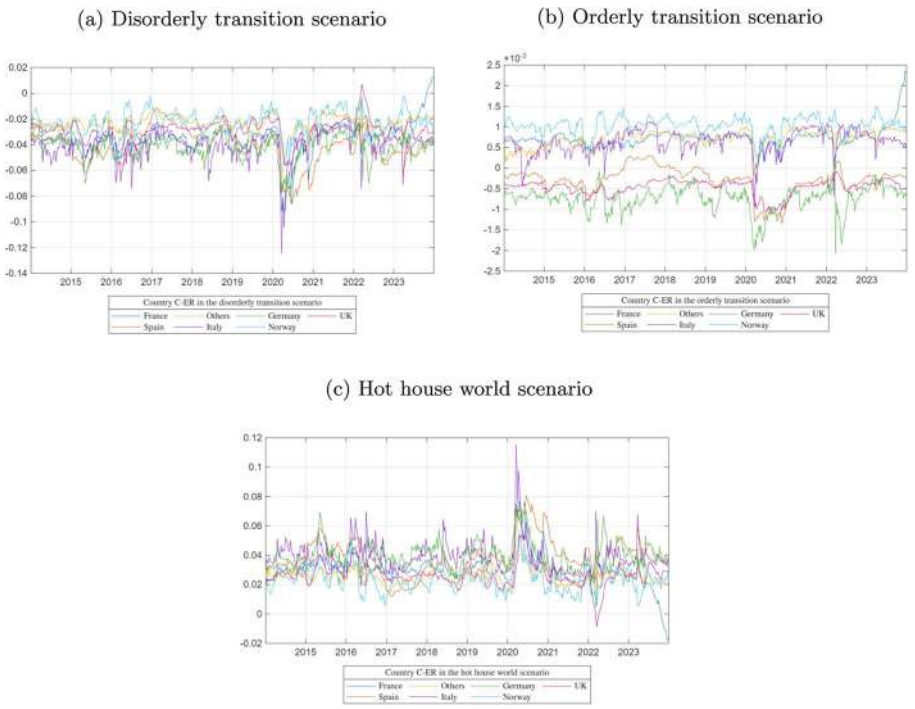

Fig. 10 Figures 10a, 10b and 10c report the C-ER for each country under orderly transition, orderly transition and hot house world scenario, respectively. The country C-ER is the mean of individual C-ER weighted for market capitalization. We have evidence of an increasing in volatility during Covid pandemic

Appendix F: Country C-VAR for disorderly transition, orderly transition and hot house world scenarios

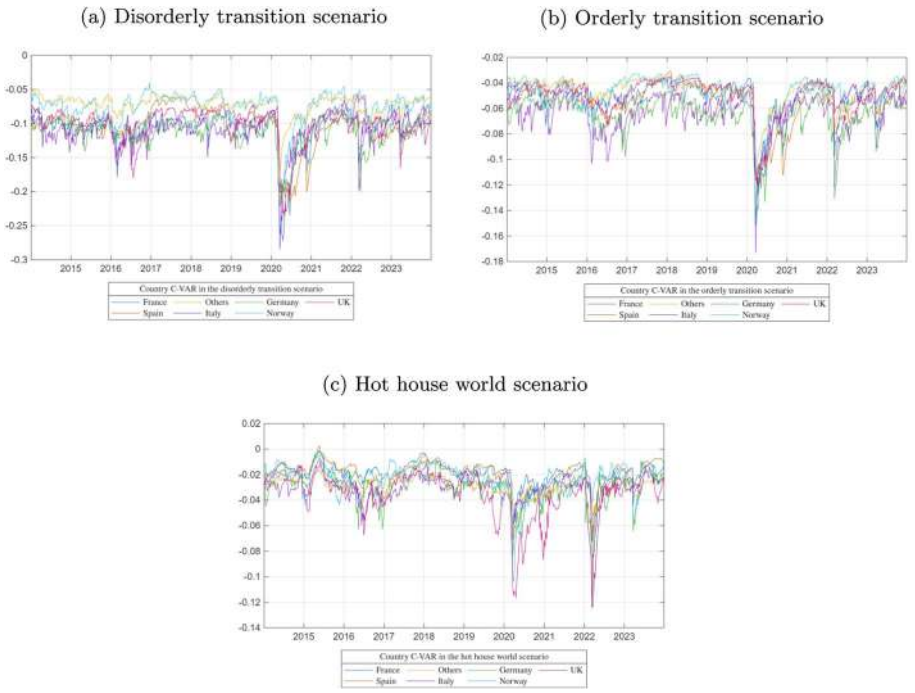

Fig. 11 Figures 11a, 11b and 11c report the C-VAR for each country under disorderly transition, orderly transition and hot house world scenario, respectively. Country C-VAR is computed as the median of individual average metrics

Appendix G: Country C-ES for disorderly transition, orderly transition and hot house world scenarios

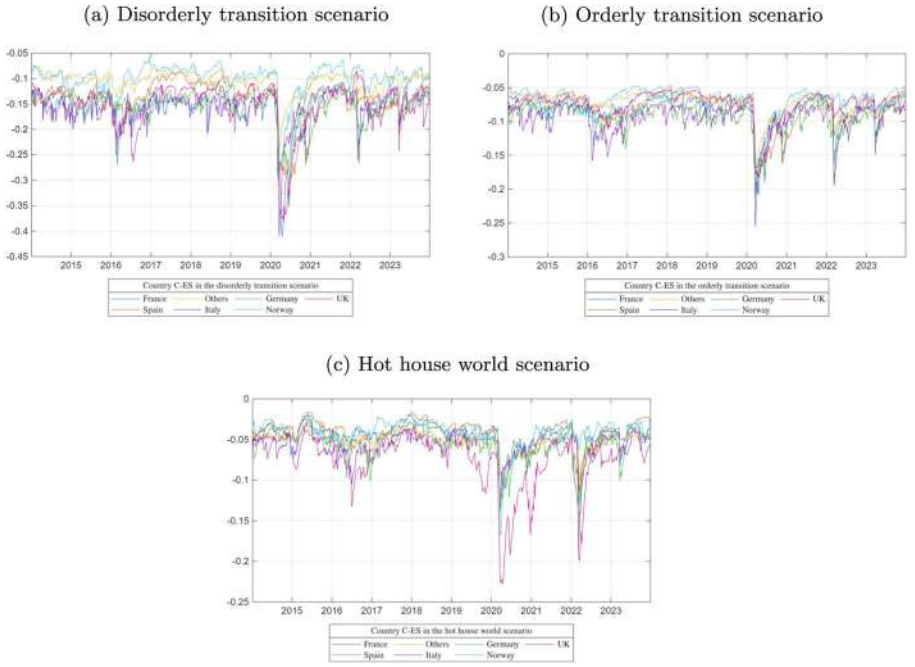

Fig. 12 Figures 12a, 12b and 12c report the C-ES for each country under orderly transition, orderly transition and hot house world scenario, respectively. Country C-ES is computed as the median of individual average metrics.

Funding Open access funding provided by Università degli Studi di Bergamo within the CRUI-CARE Agreement. This study was funded by the European Union - NextGenerationEU, in the framework of the GRINS - Growing Resilient, INclusive and Sustainable project (GRINS PE00000018 - CUP F83C22001720001). The views and opinions expressed are solely those of the authors and do not necessarily reflect those of the European Union, nor can the European Union be held responsible for them. Gabriele Torri is grateful for financial support from the Czech Scientific Foundation (GACR), Grant Number 23-07128S.

Declarations

Conflict of interest The authors have no conflicts of interest to declare that are relevant to the content of this article.

References

Acharya, V. V., Engle, R., & Richardson, M. (2012). Capital shortfall: A new approach to ranking and regulating systemic risks. *American Economic Review, 102*(3), 59–64.

Acharya, V. V., Pedersen, L. H., Philippon, T., et al. (2017). Measuring systemic risk. *The review of financial studies, 30*(1), 2–47.

Acharya, V. V., Berner, R., Engle, R., et al. (2023). Climate stress testing. *Annual Review of Financial Economics, 15*(1), 291–326.

Addoum, J. M., Ng, D. T., & Ortiz-Bobea, A. (2020). Temperature shocks and establishment sales. *The Review of Financial Studies, 33*(3), 1331–1366.

Albanese, M., Caporale, G.M., Colella, I., et al. (2024) The effects of physical and transition climate risk on stock markets: Some multi-country evidence. Tech. rep., CESifo Working Paper

Allen, D. E., Ashraf, M. A., McAleer, M., et al. (2013). Financial dependence analysis: applications of vine copulas. *Statistica Neerlandica, 67*(4), 403–435.

Allevi, E., Boffino, L., De Giuli, M. E., et al. (2019). Analysis of long-term natural gas contracts with vine copulas in optimization portfolio problems. *Annals of Operations Research, 274*, 1–37.

Alogoskoufis, S., Carbone, S., Coussens, W., et al. (2021a) Climate-related risks to financial stability. Financial stability review 1

Alogoskoufis, S., Dunz, N., Emambakhsh, T., et al. (2021b) ECB economy-wide climate stress test: Methodology and results. 281, ECB Occasional Paper

Aloui, R., Hammoudeh, S., & Nguyen, D. K. (2013). A time-varying copula approach to oil and stock market dependence: The case of transition economies. *Energy economics, 39*, 208–221.

Ardia, D., Bluteau, K., Boudt, K., et al. (2023). Climate change concerns and the performance of green vs. brown stocks. *Management Science, 69*(12), 7607–7632.

Barnett, M. (2023). Climate change and uncertainty: An asset pricing perspective. *Management Science, 69*(12), 7562–7584.

Battiston, S., Mandel, A., Monasterolo, I., et al. (2017). A climate stress-test of the financial system. *Nature Climate Change, 7*(4), 283–288.

Boirard, A., Gayle, D., Löber, T., et al. (2022) Ngfs scenarios for central banks and supervisors

Brownlees, C., & Engle, R. F. (2017). Srisk: A conditional capital shortfall measure of systemic risk. *The Review of Financial Studies, 30*(1), 48–79.

Campiglio, E., Dafermos, Y., Monnin, P., et al. (2018). Climate change challenges for central banks and financial regulators. *Nature climate change, 8*(6), 462–468.

Carney, M. (2015). Breaking the tragedy of the horizon-climate change and financial stability. *Speech given at Lloyd s of London, 29*, 220–230.

Creal, D., Koopman, S. J., & Lucas, A. (2013). Generalized autoregressive score models with applications. *Journal of Applied Econometrics, 28*(5), 777–795.

Czado, C., Bax, K., Sahin, Ö., et al. (2022). Vine copula based dependence modeling in sustainable finance. *The Journal of Finance and Data Science, 8*, 309–330.

Desnos, B., Le Guenedal, T., Morais, P., et al. (2023) From climate stress testing to climate value-at-risk: A stochastic approach. Available at SSRN 4497124

Dunz, N., Emambakhsh, T., Hennig, T., et al. (2021) Ecb's economy-wide climate stress test. ECB Occasional Paper (2021/281)

Financial Stability Board (2009) Guidance to assess the systemic importance of financial institutions, markets and instruments: Initial considerations. Tech. rep., Financial Stability Board, report to the G-20 Finance Ministers and Central Bank Governors

Giacchetta, G., Giacometti, R., et al. (2024). Measuring european banks exposure to climate risk. *Review of Corporate Finance, 4*(1–2), 151–176.

Hafner, C. M., & Manner, H. (2012). Dynamic stochastic copula models: Estimation, inference and applications. *Journal of applied econometrics, 27*(2), 269–295.

Joe, H., & Xu, J.J. (1996) The estimation method of inference functions for margins for multivariate models

Jung, H., Engle, R.F., & Berner, R. (2021) Climate stress testing. FRB of New York Staff Report (977)

Le Guenedal, T. (2022) Financial modeling of climate-related risks. PhD thesis, Institut Polytechnique de Paris

Lord, R., Bullock, S., & Birt, M. (2019) Understanding climate risk at the asset level: the interplay of transition and physical risks. S&P Global

NGFS. (2022). *Ngfs climate scenarios for central banks and supervisors*. Network for Greening the Financial System: Technical report.

Ojea-Ferreiro, J., Reboredo, J. C., & Ugolini, A. (2024). Systemic risk effects of climate transition on financial stability. *International Review of Financial Analysis, 96*, Article 103722.

Patton, A. J. (2004). On the out-of-sample importance of skewness and asymmetric dependence for asset allocation. *Journal of financial econometrics, 2*(1), 130–168.
Patton, A. J. (2006). Estimation of multivariate models for time series of possibly different lengths. *Journal of applied econometrics, 21*(2), 147–173.
Patton, A. J. (2006). Modelling asymmetric exchange rate dependence. *International economic review, 47*(2), 527–556.
Rising, J., Tedesco, M., Piontek, F., et al. (2022). The missing risks of climate change. *Nature, 610*(7933), 643–651.
Roncoroni, A., Battiston, S., Escobar-Farfán, L. O., et al. (2021). Climate risk and financial stability in the network of banks and investment funds. *Journal of Financial Stability, 54*, Article 100870.
Sautner, Z., Van Lent, L., Vilkov, G., et al. (2023). Pricing climate change exposure. *Management Science, 69*(12), 7540–7561.
Tobias, A., & Brunnermeier, M. K. (2016). Covar. *The American Economic Review, 106*(7), 1705.
Tzouvanas, P., Kizys, R., Chatziantoniou, I., et al. (2019). Can variations in temperature explain the systemic risk of european firms? *Environmental and Resource Economics, 74*(4), 1723–1759.
WMO. (2025). *State of the global climate, 2024* (p. 1368). World Meteorological Organization, WMO-No: Tech. rep.